THE FINITE ELEMENT METHOD SOLUTION OF REACTION-DIFFUSION-ADVECTION EQUATIONS IN AIR POLLUTION

ÖNDER TÜRK

SEPTEMBER 2008

THE FINITE ELEMENT METHOD SOLUTION OF REACTION-DIFFUSION-ADVECTION EQUATIONS IN AIR POLLUTION

A THESIS SUBMITTED TO
THE GRADUATE SCHOOL OF APPLIED MATHEMATICS
OF
THE MIDDLE EAST TECHNICAL UNIVERSITY

BY

ÖNDER TÜRK

IN PARTIAL FULFILLMENT OF THE REQUIREMENTS FOR THE DEGREE OF
MASTER OF SCIENCE
IN
THE DEPARTMENT OF SCIENTIFIC COMPUTING

SEPTEMBER 2008

Approval of the Graduate School of Applied Mathematics

Prof. Dr. Ersan AKYILDIZ
Director

I certify that this thesis satisfies all the requirements as a thesis for the degree of Master of Science

Prof. Dr. Bülent KARASÖZEN
Head of Department

This is to certify that we have read this thesis and that in our opinion it is fully adequate, in scope and quality, as a thesis for the degree of Master of Science.

Prof. Dr. Münevver TEZER-SEZGİN
Advisor

Examining Committee Members

Prof. Dr. Bülent KARASÖZEN _____

Prof. Dr. Münevver TEZER-SEZGİN _____

Assist. Prof. Dr. Hakan ÖKTEM _____

Assist. Prof. Dr. Ömür UĞUR _____

Instructor Dr. Ender CİĞEROĞLU _____

I hereby declare that all information in this document has been obtained and presented in accordance with academic rules and ethical conduct. I also declare that, as required by these rules and conduct, I have fully cited and referenced all material and results that are not original to this work.

Name, Last name :

Signature :

Abstract

THE FINITE ELEMENT METHOD SOLUTION OF
REACTION-DIFFUSION-ADVECTION EQUATIONS IN AIR POLLUTION

Önder Türk

M.Sc., Department of Scientific Computing

Institute of Applied Mathematics

Advisor: Prof. Dr. Münevver Tezer-Sezgin

September 2008, 71 pages

We consider the reaction-diffusion-advection (RDA) equations resulting in air pollution modeling problems. We employ the finite element method (FEM) for solving the RDA equations in two dimensions. Linear triangular finite elements are used in the discretization of problem domains. The instabilities occuring in the solution when the standard Galerkin finite element method is used, in advection or reaction dominated cases, are eliminated by using an adaptive stabilized finite element method. In transient problems the unconditionally stable Crank-Nicolson scheme is used for the temporal discretization. The stabilization is also applied for reaction or advection dominant case in the time dependent problems.

It is found that the stabilization in FEM makes it possible to solve RDA problems for very small diffusivity constants. However, for transient RDA problems, although the stabilization improves the solution for the case of reaction or advection dominance, it is not that pronounced as in the steady problems. Numerical results are presented in terms of graphics for some test steady and unsteady RDA problems. Solution of an air pollution model problem is also provided.

Keywords: FEM, Stabilized FEM, Reaction-diffusion-advection equations, Air pollution modeling.

Öz

HAVA KİRLİLİĞİNDE REAKSİYON-DİFÜZYON-ADVEKSİYON DENKLEMLERİNİN SONLU ELEMANLAR YÖNTEMİ İLE ÇÖZÜMÜ

Önder Türk

Yüksek Lisans, Bilimsel Hesaplamalar Bölümü

Uygulamalı Matematik Enstitüsü

Tez Danışmanı: Prof. Dr. Münevver Tezer-Sezgin

Eylül 2008, 71 sayfa

Bu tezde, hava kirliliği modelleme problemlerinde ortaya çıkan reaksiyon-difüzyon-adveksiyon (reaction-diffusion-advection (RDA)) denklemleri ele alınmaktadır. İki boyutlu uzayda RDA denklemlerinin çözümü için sonlu elemanlar yöntemi kullanılmaktadır. Problem tanım bölgesinin ayrıklaştırılmasında doğrusal üçgen elemanlar kullanılmaktadır. Reaksiyon veya adveksiyon baskınlığı olan durumlarda standart Galerkin sonlu elemanlar yöntemi çözümünde oluşan kararsızlıklar, uyarlanabilir stabilize edilmiş sonlu elemanlar yöntemi kullanılarak giderilmektedir. Zaman bağımlı denklemlerin çözümünde şartsız kararlı Crank-Nicolson metodu zaman boyutunda ayrık-laştırma için kullanılmaktadır. Stabilize etme yöntemi, zaman bağımlı problemlerin reaksiyon veya adveksiyon baskınlığı durumunda da kullanılmaktadır.

Stabilize edilmiş sonlu elemanlar yönteminin, çok küçük difüzyon katsayılı RDA denklemlerinin çözümünü mümkün kıldığı bulgusu elde edilmektedir. Ancak, zaman bağımlı RDA denklemlerinde stabilize etme, reaksiyon veya adveksiyon baskınlığında, çözümü iyileştirmesine rağmen zaman bağımsız problemlerdeki kadar etkili olmamaktadır. Sayısal sonuçlar zaman bağımsız ve zaman bağımlı test problemleri için grafikler yoluyla verilmektedir. Bir hava kirliliği model problemi de çözülmektedir.

Anahtar Kelimeler : Sonlu elemanlar yöntemi, Stabilize sonlu elemanlar yöntemi, Reaksiyon-difüzyon-adveksiyon denklemleri, Hava kirliliği modellemesi.

To my family

Acknowledgments

I would like to express my sincere appreciation to the members of the Institute of Applied Mathematics of Middle East Technical University, especially to Prof. Dr. Münevver TEZER-SEZGİN for her valuable guidance and helpful suggestions in every aspect from the very beginning onwards.

Deepest thanks and regards to my family who have provided me the love, support and educational background that has enabled me to be successful both in my personal and academic life.

Finally, I would also like to thank to Selçuk Han AYDIN and Alper ELALDI who have provided me the valuable support during the thesis period.

Table of Contents

List of Figures

List of Tables

Chapter 1

Introduction

The importance of the quality of atmosphere on which life exists has been recognized for the past few decades. One of the most important ways to increase the air quality is to solve the air pollution problem, mainly an optimal reduction of the air pollutants. This problem can successfully be solved with the aid of mathematical models [50]. The governing equations used in these models are reaction-diffusion-advection (RDA) equations. A non-dimensional time-independent (steady) RDA equation is written as

$$-\varepsilon\nabla^2 u + \mathbf{a}\cdot\nabla u + bu = f. \tag{1.1}$$

and a non-dimensional time-dependent (transient) RDA equation is written as

$$\frac{\partial u}{\partial t} - \varepsilon\nabla^2 u + \mathbf{a}\cdot\nabla u + bu = f \tag{1.2}$$

Here u is the solution (unknown) of the equation, $\varepsilon > 0$ is the diffusion constant, $\mathbf{a}$ is the advection vector, $b \geq 0$ is the reaction constant and f is the source term. Special cases of an RDA equation are listed below

1. If $\mathbf{a} = \vec{0}$ it is called reaction-diffusion equation
2. If $b = 0$ it is called diffusion-advection equation
3. If $\mathbf{a} = \vec{0}$ and $b = 0$ it is called diffusion equation.

Used in many fields (such as physics, chemistry, biology, geology, migration and epidemiology [20, 24]) the RDA equations have been a subject of active research and study for the last four decades and will seemingly be even more important in the next decades. However, the RDA equations and especially the systems of RDA equations cannot be solved analytically (unless some unrealistic assumptions are imposed). Therefore it is essential to solve these equations numerically. Many different methods have been proposed in the literature to solve the RDA equations numerically.

1.1 The air pollution models

The air pollution problem, particularly the reduction of air pollution to a certain level is a very important environmental problem. Air pollutants are mainly transported by advection due to the wind, diffusion and chemical reaction phenomena are also important. Therefore, this problem is not restricted to the regions where the emission sources exist, the atmosphere is polluted in the surrounding areas too. It is well known that the pollutants are dangerous for humans, plants and animals when they are over critical amounts. It is essential to reduce the air pollution to a harmless level. However, this can be a very expensive task. The critical levels are to be determined and the optimal work must be to reduce the pollution to these levels but not more as this can be very expensive. The optimal reduction of the pollutants to the desired level is a problem which can only be solved if there is a reliable mathematical model provided. The physical phenomenon of the transport of air pollution consists of three major stages which are; emission, transport of pollutants and transformations during the transport. There are both man-made and natural sources which emit different pollutants in the atmosphere. After the emission, the transport takes place. The pollutants are transported by wind. Transportation of the pollutants by wind is called advection. There are three physical processes take place during the transport of pollutants in the atmosphere.

Diffusion: The air pollutants are widely dispersed in the atmosphere in horizontal and vertical directions.

Deposition: Some of the pollutants are deposited to the various surfaces of the Earth like water, soil and plants. Usually there are two different kinds of depositions as dry deposition which is continuous and wet deposition which occurs only when it rains.

Chemical Reactions: Many different chemical reactions take place during the transport of pollutants. As a result of these reactions, many secondary pollutants are created. (The air pollutants which are emitted directly from the emission sources are called primary pollutants and the ones which come out of the reactions are called secondary pollutants). On the other hand, there are also some chemical reactions which produce harmless species. Developing a reliable mathematical model is required to be able to study the effects of the emission sources to the surrounding areas and the influence of reducing emission sources in a certain region on the pollution in the surrounding regions.

Mathematical models are essential tools to study transport of air pollutants and efficient ways of reducing the air pollution to a critical level. The most important part of modeling this transport is the mathematical description of the chemical and physical properties of the air pollutants. Therefore modeling air pollution problem needs reliable mechanisms to describe the physical and chemical properties mathematically, mathematical tools–mainly partial differential

equations–and good working numerical methods. Mathematical models of air pollution are vital tools in studying this problem. The analytical description of these large models is made by systems of partial differential equations. To begin this study one must consider the physical processes and the interactions of these processes which are emission, advection, diffusion, deposition and chemical reactions. These processes and many other important physical processes are described by a system of partial differential equations (PDE). The number of equations in such systems will be equal to the number of the species involved in the model. So, the system is huge when there are many species involved. Even when the number of the species is not very large, the discretization of the system of PDE leads to very large system of ordinary differential equations (ODE) which will be solved over a long time interval. This makes it difficult to treat these models numerically.

1.1.1 Modelling advection

The transport of various air pollutants over a long distance in the atmosphere is one of the most important physical processes that take place in long range transport of air pollution (LRTAP). It is quite sufficient to consider a single partial differential equation to express everything concerning the advection process. Obviously, the advection part of a LRTAP model does not depend on the particular air pollutants. So, we can describe the transport of any pollutants in the system by means of the same partial differential equation.

Let $u = u(x, y, z, t)$ denote the concentration of a given air pollutant at the point $(x, y, z) \in D \subset R^3$ and at a time interval [0,T] for some $T > 0$. Let $a_1 = a_1(x, y, z, t)$, $a_2 = a_2(x, y, z, t)$ and $a_3 = a_3(x, y, z, t)$ denote the wind velocities along the three coordinate axes respectively. These are assumed to be known functions defined in the whole domain D and on the whole time interval [0,T]. Now, we can describe the LRTAP pure advection by the three-dimensional PDE below

$$\frac{\partial u}{\partial t} = -\frac{\partial(a_1 u)}{\partial x} - \frac{\partial(a_2 u)}{\partial y} - \frac{\partial(a_3 u)}{\partial z} \tag{1.3}$$

for all $(x, y, z) \in D$ and for all $t \in [0, T]$.

Assuming that conservation law is satisfied for the wind velocities in the lower parts of the atmosphere as

$$\frac{\partial a_1}{\partial x} + \frac{\partial a_2}{\partial y} + \frac{\partial a_3}{\partial z} = 0 \tag{1.4}$$

we have

$$\frac{\partial u}{\partial t} = -a_1 \frac{\partial u}{\partial x} - a_2 \frac{\partial u}{\partial y} - a_3 \frac{\partial u}{\partial z} \tag{1.5}$$

for all $(x, y, z) \in D$ and for all $t \in [0, T]$.

The two-dimensional (2-D) and one-dimensional (1-D) forms of advection equations are

$$\frac{\partial u}{\partial t} = -a_1 \frac{\partial u}{\partial x} - a_2 \frac{\partial u}{\partial y} \tag{1.6}$$

and

$$\frac{\partial u}{\partial t} = -a_1 \frac{\partial u}{\partial x} \tag{1.7}$$

respectively.

The advection equation is supplied with an initial condition for having a unique solution

$$\begin{aligned} &u(x, y, z, 0) = p(x, y, z) && \text{in } 3-D \\ &u(x, y, 0) = p(x, y) && \text{in } 2-D \\ &u(x, 0) = p(x) && \text{in } 1-D. \end{aligned} \tag{1.8}$$

The advection equations stated above can generally not be solved exactly (analytically). Therefore a numerical method must be used.

1.1.2 Modelling diffusion

The other important process is the diffusion phenomenon which is the dispersion of the air pollutants in the atmosphere. To model diffusion without advection or any other process it can be assumed that the diffusion process does not depend on the pollutants so we can use the same PDE for all of the species involved in the system. It is quite sufficient here again to consider a single PDE to explain everything concerning the diffusion process as

$$\frac{\partial u}{\partial t} = \frac{\partial}{\partial x}(K_x \frac{\partial u}{\partial x}) + \frac{\partial}{\partial y}(K_y \frac{\partial u}{\partial y}) + \frac{\partial}{\partial z}(K_z \frac{\partial u}{\partial z}) \tag{1.9}$$

for all $(x, y, z) \in D$ and for all $t \in [0, T]$.

The diffusivity coefficients along the three coordinate axes are $K_x = K_x(x, y, z, t)$, $K_y = K_y(x, y, z, t)$ and $K_z = K_z(x, y, z, t)$. K_x and K_y are often assumed to be non-negative constants (e.g. $K_x = K_y = 30000 m^2/s$). K_z is more difficult to treat. (Some suggestions are on page 37 of [50]). The two-dimensional case is

$$\frac{\partial u}{\partial t} = \frac{\partial}{\partial x}(K_x \frac{\partial u}{\partial x}) + \frac{\partial}{\partial y}(K_y \frac{\partial u}{\partial y}) \tag{1.10}$$

for all $(x, y) \in D$ and for all $t \in [0, T]$.

1.1.3 Modelling deposition

It is quite sufficient to consider a single ordinary differential equation (ODE) to describe the deposition processes. Let $u_s = u_s(x, y, z, t)$ denote the concentration of the given air pollutant at the point (x, y, z) and time t. Here $s = 1, 2, ..., n$ and n is the number of pollutants studied in the model. Moreover, let $k_{1s}(x, y, t)$ denote the dry deposition coefficient and $k_{2s}(x, y, z, t)$ the wet deposition coefficient (the dry deposition does not depend on z).

The LRTAP model normally considered on space domain which is parallelepiped in the three-dimensional Euclidean space R^3. Under these assumptions made, we can describe the deposition process by the following linear ordinary differential equation (we should note here that this equation will be different in the transition from one air pollutant to another, but when the pollutant is fixed it depends only on the pollutant itself not on the others)

$$\frac{\partial u_s}{\partial t} = -(k_{1s} + k_{2s})u_s. \tag{1.11}$$

In this equation k_{1s} and k_{2s} generally depend on spatial and time variables but for some species these coefficients could be assumed to be constants. However, in each case this equation is linear and can be solved analytically. When the deposition of a given pollutant depends on the concentrations of other pollutants too, the process becomes more complicated. When this is the case, a system of ordinary differential equations must be solved. Such a system can be stated as

$$\frac{\partial u_s}{\partial t} = S_s(u_1, u_2, ..., u_n) \tag{1.12}$$

where $s = 1, 2, ..., n$.

1.1.4 Modelling chemical reactions

One of the most important processes that take place during the long range transport of air pollutants in the atmosphere is the chemistry: chemical transformations take place during the long range transport of air pollutants. Therefore the chemical reactions should be treated carefully. It is essential and highly desirable to find an optimal set which can be implemented in the model. Most of the main pollutants as sulphur pollutants, ozone, nitrogen pollutants and hydro-carbons can be used successfully in the large air pollution model. The chemical reactions involved in the long-range transport of air pollutants are listed on page 42 of [50].

1.1.5 Introduction of emissions in the model

Assume a two-dimensional model for simplicity. Let $u_i(x, y, t)$ denote the concentration of some primary air pollutants. The positions of a point (x, y) at time t are located and the emission is described by a function $E_i(x, y, t)$. The E_i functions are non-negative in general if the source of the primary pollutant exists. However, the function can sometimes be zero even when the source exists. This is the case when some sources stop emitting during the night.

1.1.6 General mathematical description of an air pollution model

A general mathematical model can easily be obtained now by combining the mathematical expressions for the five physical processes (advection, diffusion, deposition, chemical reaction and emission).

$$\begin{aligned}
\frac{\partial u_s}{\partial t} = & - \frac{\partial}{\partial x}(a_1 u_s) - \frac{\partial}{\partial y}(a_2 u_s) - \frac{\partial}{\partial z}(a_3 u_s) && \text{(advection)} \\
& + \frac{\partial}{\partial x}(K_x \frac{\partial u}{\partial x}) + \frac{\partial}{\partial y}(K_y \frac{\partial u}{\partial y}) + \frac{\partial}{\partial z}(K_z \frac{\partial u}{\partial z}) && \text{(diffusion)} \\
& - (k_{1s} + k_{2s}) u_s(x, y, z, t) && \text{(deposition)} \\
& + E_s(x, y, z, t) && \text{(emission)} \\
& + Q_s(u_1, u_2, ..., u_n) && \text{(chemistry)}
\end{aligned}$$

where $(x, y, z) \in D$, $t \in [0, T]$, $s = 1, 2, ..., n$ and n is the number of the pollutants in the model.

Any LRTAP model can be described mathematically by the system above. The number of equations in the system is equal to the number of species studied by the model. Thus, more species included in the model leads to an increase of the size of the problem. The more important fact is that the system of PDE in general cannot be solved exactly and has to be treated numerically.

There are many different numerical methods used in the treatment of large air pollution models. The system of PDE can be split into sub-systems. It is natural to split the system into parts that correspond to the physical process involved in the model. It is also natural to select the best method or the best numerical scheme for each sub-system. There are different splitting procedures that have been used in the literature [41].

If the model is three-dimensional it is convenient to perform first the computations for every horizontal plane and then to perform modifications in the vertical direction. In other words, the

first task is to split the air pollution model according to the physical processes and the second is to perform the horizontal planes computations and finally to carry out the computations along the vertical direction.

1.1.7 Horizontal planes computations

Let z_0 be fixed in $[0, Z] \subset R$, then, when the model described above is discretized, the set of points (x, y, z_0) defines a horizontal plane within the space domain of the model. Then, the computations on this horizontal plane are carried out by treating numerically the four systems

$$\begin{aligned}
\frac{\partial u_s^{(1)}}{\partial t} &= -\frac{\partial (a_1 u_s^{(1)})}{\partial x} - \frac{\partial (a_2 u_s^{(1)})}{\partial y} \\
\frac{\partial u_s^{(2)}}{\partial t} &= \frac{\partial}{\partial x}(K_x \frac{\partial u_s^{(2)}}{\partial x}) + \frac{\partial}{\partial y}(K_y \frac{\partial u_s^{(2)}}{\partial y}) \\
\frac{\partial u_s^{(3)}}{\partial t} &= -(k_{1s} + k_{2s}) u_s^{(3)}(x, y, z_0, t) \\
\frac{\partial u_s^{(4)}}{\partial t} &= E_s(x, y, z_0, t) + Q_s(u_1^{(4)}, u_2^{(4)}, ..., u_n^{(4)})
\end{aligned} \tag{1.13}$$

where $s = 1, 2, ..., n$.

1.1.8 Vertical lines computations

Assume that (x_0, y_0) is a fixed point with x_0 in $[0, X] \subset R$ and y_0 in $[0, Y] \subset R$. When the model is discretized, the set of points (x_0, y_0, z) defines a vertical grid-line within the space domain of the model. Then the computations for (x, y) can be carried out by treating the following system numerically

$$\frac{\partial u_s^{(5)}}{\partial t} = -\frac{\partial}{\partial z}(a_3 u_s^{(5)}) + \frac{\partial}{\partial z}(K_z \frac{\partial u_s^{(5)}}{\partial z}) \tag{1.14}$$

where again $s = 1, 2, ..., n$. We see that the system of PDE's can be split into five PDE systems and solved separately at every time step. Then the five systems must be coupled. The process of coupling the systems arising after the splitting of the model can be carried out in the following way. At each time step, the five systems are solved successively. When the concentrations u_s at time t are found, the first system is solved using the approximations of u_s as starting values. The solution found is used as a starting vector in the treatment of the second system. This

process is continued by taking the solution of the third system is used as a starting vector in the treatment of the fourth system and the solution of the fourth system is used in the treatment of the fifth system. Finally, the approximated solution of the fifth system is accepted as an approximation to the solution of the global model at time $t + \Delta t$ (where Δt is the time step size) and thus, the next time step starts in the same way.

1.2 A review of methods used to solve reaction-diffusion-advection (RDA) equation

Solving the RDA equation has attracted much interest for long time. There are many approaches and studies in the literature. We give a review of them in the historical order below. Molenkamp [42] calculated numerical solutions to the advection equation in 1967 using finite-difference approximations and has shown that Roberts-Weiss approximation worked well but requires 10-40 times more time than any other schemes considered (Upstream, Leap-frog, Lax-Wendroff, Arakawa-Euler and Arakawa-Adams-Bashforth).

Long and Pepper [40] analyzed the donor cell, fully implicit, Crank-Nicolson, quasi-Lagrangian, second moment and linear finite element methods for calculation of scalar advection equation and summarized that each scheme exhibited certain disadvantages.

It has been recognized that when advection or reaction dominates diffusion, some physical effects take place in the problem on a scale which is very small but having a strong impact on the larger scales. Therefore, they cause an unfeasible solution when a standard Galerkin finite element method (SGFEM) is used. The streamline upwind Petrov-Galerkin (SUPG) method, proposed by Brooks and Hughes [12], was the first variationally consistent, stable and accurate finite element model for advection-dominated problems. This method initialized the development of stabilization techniques for advection-dominated problems and the theory has been developed over the years. The stabilized finite element methods are formed by adding variational mesh-dependent, consistent and numerically stabilizing terms to the standard Galerkin method. These methods have the desirable properties of improving the numerical stability of the Galerkin method and of preserving good accuracy. Tezduyar and Park [46] presented formulations which complement the SUPG method to minimize the oscillations about sharp internal and boundary layers in advection-dominated and reaction-dominated flows. Later on, the Galerkin-Least-Squares (GLS) version was introduced [34] and a few years later, an unusual version of the stabilized methods was introduced by Franca and Farhat [26].

The Galerkin method using low-order piecewise polynomials perform poorly for advection-dominated equations. Adding terms to the variational formulation is a well accepted practice, as it is done using stabilized methods. It was rather unexpected that the Galerkin method

without additional terms can be used as a starting point for these problems as well. In [10] a relationship is established between the Galerkin method enriched with bubble functions and the stabilized method described in [25] for diffusion-advection equations. If inappropriate choices of bubbles are taken, then the Galerkin method performs as a disguised stabilized method with the wrong selection of the stability parameter. To treat this pathology, special bubble designs were suggested [10, 11, 27, 44]. Among them, residual-free bubbles take into account the partial differential equation being approximated, in the generation of the enrichment space being added to the finite element piecewise polynomial space. Although residual-free bubbles form a framework to derive improved discretizations, it was still needed to compute residual-free basis functions by solving partial differential equations at the element level. Some progress has been made in approximating these computations and furthermore Franca and Valentin [30] avoided these difficulties by pursuing an improved unusual stabilized method (USFEM) given in [26]. Herein, they used a mesh parameter inspired by residual-free bubbles, as part of the new stability parameter design. They demonstrated that improved numerical results can be attained with the USFEM for RDA equations, by carefully revisiting the definition of the stability parameter. They took USFEM as the starting point and by looking at three asymptotic limits (for high advection, diffusion and reaction), they designed a newer parameter that has superior numerical performance and preserving the global convergence error estimating rates that were obtained earlier.

Cannon and Lin [15] studied finite element method approximations to the nonlinear diffusion equations using the so called priori L^2-Error-Estimates method.

Lanser and Verwer [37] analyzed the operator or time splitting in the numerical solution of initial boundary value problems for differential equations to study computational air pollution modelling. They concluded that in most applications splitting errors would occur and in air pollution models the splitting error would oscillate and would not grow beyond bound for evolving time.

Franca, Nesliturk and Stynes [28] considered the application of residual-free bubble functions to solve diffusion-advection problems in two dimensions and showed that the method is as stable as the streamline diffusion method (SDFEM/SUPG). They also studied an application of the two-level finite element method for the diffusion-advection equation which was introduced in [29] for the Helmholtz equation.

Chawla, Al-Zanaidi and Al-Aslab [16] described a one-parameter family of unconditionally stable third-order time integration schemes based on the extended trapezoidal formulas for the diffusion-advection equation.

Baumann and Oden [7] presented a new method called discontinuous hp finite element method for diffusion-advection problems.

Verwer, Hundsdorfer and Blom [49] reported that due to the large number of chemical species and the three space dimensions, off-the-shelf stiff ODE integrators are not feasible for the numerical time integration of stiff systems of RDA equations from the field of air pollution modelling. They performed a survey of special time integration techniques, encompassing stiff chemistry solvers, positive advection schemes, time or operator splitting, implicit-explicit methods and approximate matrix factorization solutions. They also reported on experiences with vector/parallel shared memory and massively parallel distributed memory architectures and clusters of workstations for solving huge problem scales.

Recently Franca, Hauke and Masud [31] revisited the stabilized finite element methods and illustrated the development of the methods applied to diffusion-advection problems.

Fang [23] solved initial and boundary value problems of diffusion-advection equations in a square region by using finite difference approximations with respect to spatial variables and an implicit method with respect to the time variable. It was shown that the numerical solution is convergent if the derivatives go to infinity under proper conditions and the convergence of numerical solution can be accelerated if the mesh points are some functions of equidistant mesh points.

Alexandrov and Zlatev [1] stated that large-scale air pollution models can successfully be used in different environmental studies. These models are described mathematically by systems of partial differential equations. Splitting procedures followed by discretization of the spatial derivatives lead to several large systems of ordinary differential equations of order up to 80 millions. They added that many scenarios are often to be run in order to study the dependence of the model results on the variation of some key parameters (as, for example, the emissions). Such huge computational tasks can successfully be treated only if fast and sufficiently accurate numerical methods are used and the models can efficiently be run on parallel computers. They presented efficient Monte Carlo methods for some subproblems and showed applications of the model in the solution of some environmental tasks. A similar study was performed in [2, 21].

Caliari, Vianello and Bergamaschi [14] implemented a second-order exponential integrator for semidiscretized RDA equations, obtained by coupling exponential-like Euler and Midpoint integrators. They did numerical tests on two-dimensional models discretized in space by Finite Differences or Finite Elements and showed that their method can be up to 5 times faster than a classical second-order implicit solver.

Knobloch [36] considered the Mizukami-Hughes method for the numerical solution of scalar two-dimensional steady diffusion-advection equations using conforming triangular piecewise linear finite elements and proposed several modifications of this method to eliminate its shortcomings. It was reported that this method gives very accurate discrete solutions in advection-dominated problems and showed how the Mizukami-Hughes method can be applied to RDA

equations and to three-dimensional problems.

Tian and Dai [47] proposed a class of high-order compact (HOC) exponential finite difference (FD) methods for solving one-dimensional and two-dimensional steady-state diffusion-advection problems. They stated that the newly proposed HOC exponential FD schemes have nonoscillation property and yield high accuracy approximation solution. They also compared analytical solutions and numerical results for the proposed HOC exponential FD methods and some previously published HOC methods.

Bozkaya [9] used least-squares differential quadrature method (DQM) for solving the ordinary differential equations in time, obtained from the application of dual reciprocity boundary element method (DRBEM) for the spatial partial derivatives in diffusion-advection problems. The DRBEM enabled the use of fundamental solution of Laplace equation, which is easy to implement computationally. The terms except the Laplacian were considered as the nonhomogeneity in the equation, which are approximated in terms of radial basis functions. The application of DQM for time derivative discretization when it was combined with the DRBEM gave an overdetermined system of linear equations since both boundary and initial conditions were imposed. The least squares approximation was used for solving the overdetermined system. Thus, the solution is obtained at any time level without using an iterative scheme and numerical results in good agreement with the theoretical solutions of the diffusion-advection problems obtained.

John, Kaya and Layton [35] studied the error in the efficient implementation of time stepping methods for a variational multiscale method (VMS) for solving advection-dominated problems. They observed that the global accuracy of the most straightforward VMS implementation was much better than the artificial diffusion stabilization and comparable to a streamline-diffusion finite element method in the tests.

Asensio, Ayuso and Sangalli [5] presented some numerical schemes for the unsteady RDA linear problems, investigated two possible different ways of combining the discretization in time and in space. Discretization in time was performed by using the Crank-Nicolson finite difference scheme, while for the space discretization they considered classical stabilized finite element schemes.

Chou, Zhang, Zhao and Nie [18] studied a linearly unconditionally stable method that approximates both diffusions and reactions implicitly using a second order Crank-Nicholson scheme. The nonlinear system resulted from the implicit approximation at each time step was solved using a multi-grid method. Numerical simulations performed in this study demonstrated that the method is accurate and robust with convergence using even very large size of time steps.

Gravemeier and Wall [33] proposed a multiscale method for the numerical solution of transient RDA equations. A particular feature of the method was that no large matrix system has

to be solved. Numerical tests performed in the study showed that for both problematic flow regimes (the regime of dominant advection and the regime of dominant advection and absorption) the presented method provided completely stable solutions, which were not achieved by standard stabilized methods. A shortcoming of the proposed method was noted which is that the method revealed itself in a too smooth resolution of regions with a sharp gradient in the solution field

Gracia and Lisbona [32] considered a system of two parabolic singularly perturbed equations of reaction-diffusion. The asymptotic behaviour of the solution and its partial derivatives was given. A decomposition of the solution in its regular and singular parts used for the asymptotic analysis of the spatial derivatives. To approximate the solution they considered the implicit Euler method for time stepping and the central difference scheme for spatial discretization on a special piecewise uniform Shishkin mesh. They proved that this scheme is uniformly convergent, with respect to the diffusion parameters, having first-order convergence in time and almost second-order convergence in space, in the discrete maximum norm. Numerical experiments are illustrated and the order of convergence is proved theoretically.

Bermejo and Carpio [8] introduced an adaptive method that combines a semi-Lagrangian scheme with a second order implicit-explicit Runge-Kutta-Chebyshev (IMEX-RKC) method to calculate the numerical solution of advection dominated reaction-diffusion problems. The advection terms were integrated via the semi-Lagrangian scheme, whereas the IMEX-RKC treated the diffusion terms explicitly and the highly stiff reaction terms implicitly in this study. The space adaptation was done in the framework of finite elements and the criterion for adaptation was derived from the information supplied by the semi-Lagrangian step.

In this thesis we have considered the reaction-diffusion-advection problems which are in general resulting from the air pollution problems. The method employed is the finite element method with linear triangular elements. The stabilization techniques from [4] are used whenever necessary for small diffusivity constants. For transient RDA equations the Crank-Nicolson scheme is made use of for time integration. Numerical results are obtained for some test problems in steady and transient cases. It has been found that the stabilization in FEM application is more effective in the steady problems for very small diffusivity constant. In the transient problems the effect of stability is not that pronounced. A test problem is included from the air pollution problems which is defined with the diffusion-reaction equation.

Chapter 2

Finite Element Method Solution of Reaction-Diffusion-Advection Equations

In this chapter, we describe the finite element method and a stabilized finite element method introduced in [4] for solving the reaction-diffusion-advection (RDA) equation. The methods are described for a two-dimensional model problem.

The finite element method (FEM) is a powerful numerical tool for solving algebraic, differential and integral equations. It is more general and more powerful then the finite difference method. The method has three important features which make it superior over other competitive methods. First, a domain which is geometrically complex of the problem can be represented as a collection of simpler subdomains which are called finite elements. Second, the algebraic equations developed using the governing equations of the problem are solved over each finite element. Third, the equations and relationships from all elements are assembled so as to be put back into their original positions in the whole domain of the problem. Therefore this method is more powerful in its application to real world problems that involve physics geometry and boundary conditions. In the finite element method, we seek an approximation u_h to the solution u in the form

$$u \approx u_h = \sum_{j=1}^{n} u_j \psi_j \tag{2.1}$$

where u_j are the values of u_h at the element nodes, ψ_j are the interpolation functions and n is the number of the nodes in one element. Direct substitution of such approximations into the governing differential equations does not generally result in a necessary and sufficient number of equations for the undetermined coefficients u_j. Therefore a weighted-integral form of the governing equation is used to obtain a necessary and sufficient number of equations.

2.1 FEM for two dimensional (RDA) problems

We consider the model equation

$$-\varepsilon\nabla^2 u + \mathbf{a}\cdot\nabla u + bu = f \qquad \text{in } \Omega \tag{2.2}$$

with some specified boundary conditions on the boundary Γ of the domain Ω.

Here $\nabla^2 u = \dfrac{\partial^2 u}{\partial x^2} + \dfrac{\partial^2 u}{\partial y^2}$, $\mathbf{a} = (a_1, a_2)$ and $\mathbf{a}\cdot\nabla u = a_1\dfrac{\partial u}{\partial x} + a_1\dfrac{\partial u}{\partial y}$.

The major steps developing the finite element model are [43]

1. Discretization of the domain into a set of finite elements.
2. Weak or weighted-integral formulation of the governing equation.
3. Derivation of finite element interpolating functions.
4. Development of the finite element method via the weak form.
5. Assembly of finite elements.
6. Imposition of boundary conditions.
7. Solution of the system of algebraic equations obtained.

Discretization

In two dimensional problems there are many geometric shapes that can be used as finite elements as it can be seen in Figure 2.1.

In such irregular domains, the discretization of the domain into simpler subdomains brings an error from the approximation of the domain. In our present study, however, we used a square as the domain of the problem and therefore, the error coming from approximation of the domain is annihilated. We used identical linear triangle elements (triangles with three nodes as vertices) in all of the problems we study in this thesis.

Weak or weighted-integral formulation

We are going to consider only a typical element in developing the weak form. We take Ω_e as a typical element and will develop the finite element model of (2.2) over Ω_e. First, multiply (2.2) with a weight function w (which is assumed to be differentiable once with respect to x and y) then integrate the equation over the element Ω_e

$$\int_{\Omega_e} w(-\varepsilon\nabla^2 u + \mathbf{a}\cdot\nabla u + bu - f)dxdy = 0. \tag{2.3}$$

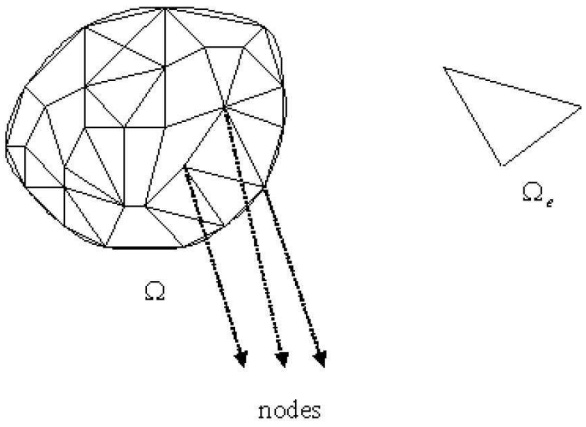

Figure 2.1: Discretization

Applying the divergence theorem we obtain

$$\int_{\Omega_e} (\varepsilon \nabla w \nabla u + w(\mathbf{a} \cdot \nabla u) + bwu - wf)dxdy - \oint_{\Gamma_e} \varepsilon w(\mathbf{n} \cdot \nabla u)ds = 0. \tag{2.4}$$

where $\mathbf{n} = (n_x, n_y)$ is the unit normal vector on the boundary Γ_e.

From the boundary integral in (2.4) one can see that the specification of u comprises the necessary boundary conditions, and thus u is the main variable.

The coefficient of the weight function in the boundary expression is

$$q_n = \varepsilon(\mathbf{n} \cdot \nabla u) = n_x(\varepsilon \frac{\partial u}{\partial x}) + n_y(\varepsilon \frac{\partial u}{\partial y}). \tag{2.5}$$

The specification of q_n constitutes the natural boundary condition, therefore q_n is the secondary variable. The normal n is taken positive outward from the surface on the boundary of the element, namely on Γ_e.

Finally, from (2.4) and (2.5) we obtain the weak form of (2.2)

$$\int_{\Omega_e} (\varepsilon \nabla w \nabla u + w(\mathbf{a} \cdot \nabla u) + bwu - wf)dxdy - \oint_{\Gamma_e} wq_n ds = 0. \tag{2.6}$$

Using bilinear form $B^e(\cdot, \cdot)$ and linear form $l^e(\cdot)$ we can write (2.6) equivalently as

$$B^e(w, u) = l^e(w) \tag{2.7}$$

where

$$B^e(w, u) = \int_{\Omega_e} (\varepsilon \nabla w \nabla u + w(\mathbf{a} \cdot \nabla u) + bwu)dxdy \tag{2.8}$$

and

$$l^e(w) = \int_{\Omega_e} wf dxdy + \oint_{\Gamma_e} wq_n ds. \tag{2.9}$$

Finite Element Model

The weak form in equation (2.6) requires that the approximation for u should be at least linear in x and y so that the terms in (2.4) are nonzero. The Lagrange interpolating functions are admissible as the primary variable is the function itself.

Let u be approximated over a finite element Ω_e by [43]

$$u(x,y) \approx u_h^e(x,y) = \sum_{j=1}^{n} u_j^e \psi_j^e(x,y) \tag{2.10}$$

where u_j^e is the value of u_h^e at the jth node (x_j, y_j) of the element and ψ_j^e are the Lagrange interpolation functions with the following property

$$\psi_i^e(x_j, y_j) = \delta_{ij} = \begin{cases} 1 & \text{if} \quad i = j \\ 0 & \text{if} \quad i \neq j \end{cases}$$

where $i, j = 1, 2, ..., n$.

Deriving the finite element equations in algebraic form does not depend on the shape of the element Ω_e or on the form of $\psi_i^e(x_j, y_j)$. Later on we are going to derive the specific form of $\psi_i^e(x_j, y_j)$ for linear triangular elements in our study. (Once again we note that higher order elements and other shapes can also be used).

Now substituting the finite element approximation (2.10) of u into the weak form in equation (2.6) we obtain

$$\begin{aligned} \int_{\Omega_e} \Bigg\{ \varepsilon \left(\frac{\partial w}{\partial x} \sum_{j=1}^{n} u_j^e \frac{\partial \psi_j^e}{\partial x} + \frac{\partial w}{\partial y} \sum_{j=1}^{n} u_j^e \frac{\partial \psi_j^e}{\partial y} \right) + a_1 w \sum_{j=1}^{n} u_j^e \frac{\partial \psi_j^e}{\partial x} + a_2 w \sum_{j=1}^{n} u_j^e \frac{\partial \psi_j^e}{\partial y} \\ + bw \sum_{j=1}^{n} u_j^e \psi_j^e - wf \Bigg\} dxdy - \oint_{\Gamma_e} wq_n ds = 0. \end{aligned} \tag{2.11}$$

This equation must hold for every admissible weight function w. We need n linearly independent algebraic equations to solve for the n unknowns, $u_1^e, u_2^e, ..., u_n^e$, so we choose the same linearly independent interpolation functions for w as $\psi_1^e, \psi_2^e, ..., \psi_n^e$ which gives the Galerkin method.

The ith algebraic equation obtained by substituting $w = \psi_i^e$ into (2.11) is

$$\sum_{j=1}^{n}[\int_{\Omega_e}\left\{\varepsilon\left(\frac{\partial\psi_i^e}{\partial x}\frac{\partial\psi_j^e}{\partial x}+\frac{\partial\psi_i^e}{\partial y}\frac{\partial\psi_j^e}{\partial y}\right)+a_1\psi_i^e\frac{\partial\psi_j^e}{\partial x}\right.$$
$$\left.+a_2\psi_i^e\frac{\partial\psi_j^e}{\partial y}+b\psi_i^e\psi_j^e\right\}dxdy]u_j-\int_{\Omega_e}f\psi_i^e dxdy-\oint_{\Gamma_e}\psi_i^e q_n ds=0 \tag{2.12}$$

where $i=1,2,...,n$.

Observe that (2.12) can be put into the form

$$\sum_{j=1}^{n}K_{ij}^e u_j^e=f_i^e+Q_i^e \qquad\qquad i=1,2,...,n \tag{2.13}$$

where

$$K_{ij}^e=\int_{\Omega_e}\left\{\varepsilon\left(\frac{\partial\psi_i^e}{\partial x}\frac{\partial\psi_j^e}{\partial x}+\frac{\partial\psi_i^e}{\partial y}\frac{\partial\psi_j^e}{\partial y}\right)+a_1\psi_i^e\frac{\partial\psi_j^e}{\partial x}+a_2\psi_i^e\frac{\partial\psi_j^e}{\partial y}+b\psi_i^e\psi_j^e\right\}dxdy$$

$$f_i^e=\int_{\Omega_e}f\psi_i^e dxdy \tag{2.14}$$

$$Q_i^e=\oint_{\Gamma_e}\psi_i^e q_n ds.$$

In matrix notation, equation (2.13) takes the form

$$[K^e]\{u^e\}=\{f^e\}+\{Q^e\}. \tag{2.15}$$

This equation represents the finite element model of (2.2) where $[K^e]$ is an $n\times n$ element symmetric matrix, $\{f^e\}$ and $\{Q^e\}$ are $n\times 1$ element vectors.

Interpolating Functions

The finite element approximation $u_h^e(x,y)$ over a typical element Ω_e converges to the true solution if the following conditions are satisfied:

1. u_h^e must be continuous.
2. The polynomials used to represent u_h^e must be complete (i.e., all terms up to the highest-order should be included in u_h^e).
3. All the terms of the polynomials should be linearly independent.

The number of linearly independent terms in the u_h^e representation designates the number of degrees of freedom and the shape of the element.

Triangular Element

As we mentioned before, ψ_i^e should be at least linear in x and y. Therefore, the complete linear polynomial in the element Ω_e must be of the form [43]

$$u_h^e(x,y) = c_1^e + c_2^e x + c_3^e y \tag{2.16}$$

where c_i^e are constants. In a typical linear triangular element, the nodes are the vertices of the triangle. However, this is not necessary, and the nodes can also be located on the sides of the triangle.

The equation (2.16) defines a unique plane which means that if $u(x,y)$ is a curved surface, $u_h^e(x,y)$ approximates the surface by a plane. $u_h^e(x,y)$ is uniquely defined on a triangle by the three values at the vertices of the triangle.

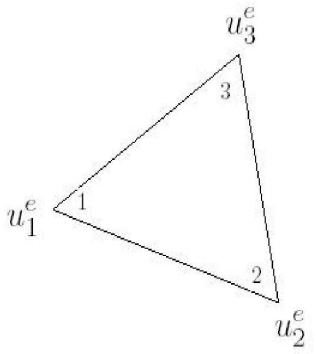

The three constants c_1^e, c_2^e and c_3^e can be expressed in terms of nodal values u_1^e, u_2^e and u_3^e. Therefore the polynomial in (2.16) correlated with the triangle element and there are three nodes identified which are the vertices of the triangle. Equations take the form

$$\begin{aligned} u_1^e &= u_h^e(x_1,y_1) = c_1 + c_2 x_1 + c_3 y_1 \\ u_2^e &= u_h^e(x_2,y_2) = c_1 + c_2 x_2 + c_3 y_2 \\ u_3^e &= u_h^e(x_3,y_3) = c_1 + c_2 x_3 + c_3 y_3 \end{aligned} \tag{2.17}$$

dropping the superscript 'e' for simplicity. Solving these equations for c_1, c_2 and c_3 we obtain

$$\begin{aligned} c_1 &= \frac{1}{2A}(\alpha_1 u_1 + \alpha_2 u_2 + \alpha_3 u_3) \\ c_2 &= \frac{1}{2A}(\beta_1 u_1 + \beta_2 u_2 + \beta_3 u_3) \\ c_2 &= \frac{1}{2A}(\gamma_1 u_1 + \gamma_2 u_2 + \gamma_3 u_3) \end{aligned} \tag{2.18}$$

where A is the area of the element with vertices (x_i, y_i) $(i = 1, 2, 3)$ and $\alpha_i, \beta_i, \gamma_i$ are as follows

$$\begin{aligned} \alpha_1 &= x_2y_3 - x_3y_2 \qquad \beta_1 = y_2 - y_3 \qquad \gamma_1 = x_3 - x_2 \\ \alpha_2 &= x_3y_1 - x_1y_3 \qquad \beta_2 = y_3 - y_1 \qquad \gamma_2 = x_1 - x_3 \\ \alpha_3 &= x_1y_2 - x_2y_1 \qquad \beta_3 = y_1 - y_2 \qquad \gamma_3 = x_2 - x_1. \end{aligned} \tag{2.19}$$

Substituting c_i into (2.16) we obtain

$$u_h^e(x, y) = \textstyle\sum_{i=1}^{3} u_i^e \psi_i^e(x, y) \tag{2.20}$$

where ψ_i^e are the linear interpolating functions for the triangular element

$$\psi_i^e = \tfrac{1}{2A_e}(\alpha_i^e + \beta_i^e x + \gamma_i^e y) \qquad i = 1, 2, 3 \tag{2.21}$$

and A_e is the area of the triangle element Ω_e.

Evaluation of Element Matrices for a Linear Triangular Element

The matrices $[K^e]$ and $\{f^e\}$ given in equation (2.15) generally cannot be evaluated exactly and thus they have to be calculated numerically. However, when ε, a_1, a_2 and b are constants elementwise, it's possible to evaluate the integrals exactly over the triangular element. The boundary integral $\{Q^e\}$ can be evaluated when q_n is known. For the interior elements which don't have any of its sides on the boundary of the problem, the contribution from the boundary integral cancels with similar contributions from adjoining elements.

When ε, a_1, a_2 and b are constants elementwise, we can rewrite K_{ij}^e in (2.14) as

$$K_{ij}^e = \varepsilon[S_{ij}^e] + a_1[P1_{ij}^e] + a_2[P2_{ij}^e] + b[M_{ij}^e] \qquad i, j = 1, 2, 3 \tag{2.22}$$

where

$$\begin{aligned} S_{ij}^e &= \int_{\Omega_e} \left(\frac{\partial \psi_i^e}{\partial x} \frac{\partial \psi_j^e}{\partial x} + \frac{\partial \psi_i^e}{\partial y} \frac{\partial \psi_j^e}{\partial y} \right) dxdy \\ P1_{ij}^e &= \int_{\Omega_e} \psi_i^e \frac{\partial \psi_j^e}{\partial x} dxdy \\ P2_{ij}^e &= \int_{\Omega_e} \psi_i^e \frac{\partial \psi_j^e}{\partial y} dxdy \\ M_{ij}^e &= \int_{\Omega_e} \psi_i^e \psi_j^e dxdy. \end{aligned} \tag{2.23}$$

The integrals of polynomials can be evaluated exactly over triangular domains and given by the formulae below

$$S_{ij}^e = \frac{1}{4A_e}(\beta_i\beta_j + \gamma_i\gamma_j)$$

$$P1_{ij}^e = \frac{\beta_j}{6}$$

$$P2_{ij}^e = \frac{\gamma_j}{6}$$

$$M_{ij}^e = \frac{1}{4A_e}\left\{\alpha_i\alpha_j + \frac{1}{3}\left(\alpha_i\beta_j + \alpha_j\beta_i\right)\left(x_1 + x_2 + x_3\right) + \frac{1}{3}\left(\alpha_i\gamma_j + \alpha_j\gamma_i\right)\left(y_1 + y_2 + y_3\right) + I\right\} \tag{2.24}$$

where

$$I = \frac{1}{A_e}[I_1\beta_i\beta_j + I_2(\gamma_i\beta_j + \gamma_j\beta_i) + I_3\gamma_i\gamma_j] \tag{2.25}$$

and

$$I_1 = \frac{A_e}{12}\left[\left(x_1^2 + x_2^2 + x_3^2\right) + \left(x_1 + x_2 + x_3\right)^2\right]$$

$$I_2 = \frac{A_e}{12}\left[x_1y_1 + x_2y_2 + x_3y_3 + \left(x_1 + x_2 + x_3\right)\left(y_1 + y_2 + y_3\right)\right] \tag{2.26}$$

$$I_3 = \frac{A_e}{12}\left[\left(y_1^2 + y_2^2 + y_3^2\right) + \left(y_1 + y_2 + y_3\right)^2\right].$$

In addition, if $f = f_e$ is constant on the element Ω_e then

$$f_i^e = \int_{\Omega_e} f_e\psi_i^e dxdy = \frac{1}{3}f_eA_e. \tag{2.27}$$

The next step after the evaluation of all element matrices is the assembly of elements. The assembly of finite elements is carried out by imposing interelement continuity of primary variable and balance of secondary variable. Finally, the boundary conditions are imposed to the system and the final algebraic system

$$K^*U = Q^* \tag{2.28}$$

is solved for U to obtain the unknown values of the problem on the nodes. U is the vector containing nodal values of u_h, and K^* and Q^* are the global matrices assembled from the matrix K_{ij}^e and vectors $f_i^e + Q_i^e$ respectively.

2.1.1 An adaptive stabilized finite element method

The standard Galerkin approximation usually introduces nonphysical oscillations when the problem is either advection or reaction dominated. One way to solve this problem is to add some numerical diffusion terms to the variational formulation. These terms stabilize the finite element solution and therefore, a stabilized finite element method is obtained. There are many possible choices of such terms. We use the adaptive scheme introduced in [4]. The scheme is obtained by combining the stabilized finite element method introduced in [30] and an error estimator using constants which only depends on the mesh. It is reported that this scheme attains an optimal order of convergence (see [4] for details).

The variational formulation of the RDA equation in (2.2) is given in (2.7) as

$$B^e(w,u) = l^e(w). \tag{2.29}$$

The stabilized formulation now is [4]

$$B^e_\tau(w,u) = l^e_\tau(w) \tag{2.30}$$

where

$$B^e_\tau(w,u) = B^e(w,u) + \sum \int_{\Omega_e} \tau_K(-\varepsilon\nabla^2 w - \mathbf{a}\cdot\nabla w + bw)(-\varepsilon\nabla^2 u + \mathbf{a}\cdot\nabla u + bu)dxdy \tag{2.31}$$

and

$$l^e_\tau(w) = l^e(w) - \sum \int_{\Omega_e} \tau_K f(-\varepsilon\nabla^2 w - \mathbf{a}\cdot\nabla w + bw)dxdy. \tag{2.32}$$

Here summations are all over Ω_e.

The stabilization parameter τ_K is defined as follows [4]

$$\tau_K = \frac{h_K^2}{bh_K^2 max\left\{1, Pe_K^R\right\} + (2\varepsilon/m_k)\, max\left\{1, Pe_K^A\right\}} \tag{2.33}$$

where

$$Pe_K^R = \frac{2\varepsilon}{m_k b h_K^2} \qquad \text{and} \qquad Pe_K^A = \frac{m_k|\mathbf{a}|h_K}{\varepsilon} \tag{2.34}$$

with $|\mathbf{a}| = \sqrt{a_1^2 + a_2^2}$.

The τ_K formula has a form that is suggested by static condensation along with two switches for the asymptotic behavior of the reaction, diffusion coefficients and the norm of the advection vector, [30]. The comparison between these coefficients is performed by Pe_K^R and Pe_K^A. The final parameter τ_K reflects the asymptotic behavior under any limiting case. In our study, we take $m_k = 1/3$. The parameter h_K is a measure of the element size. It is reported that under the presence of advection, the element parameter h_K that yields the best numerical results is

computed using the largest streamline distance in the element. The computation of h_K using this idea is suggested by residual-free-bubbles. (Detailed information about m_k and h_K can be obtained from [4, 30]).

We note that since we use linear elements we have $\nabla^2 u_h = 0$ and $\nabla^2 w = 0$. Therefore, equations in (2.31) and (2.32) now become simpler as

$$B_\tau^e(w,u) = B^e(w,u) + \sum \int_{\Omega_e} \tau_K(-\mathbf{a}\cdot\nabla w + bw)(\mathbf{a}\cdot\nabla u + bu)dxdy \tag{2.35}$$

and

$$l_\tau^e(w) = l^e(w) - \sum \int_{\Omega_e} \tau_K f(-\mathbf{a}\cdot\nabla w + bw)dxdy \tag{2.36}$$

respectively.

2.2 Numerical Results

In this section we present some test problems and solve them by using finite element method or the stabilized finite element method described above. We work on four test problems (1) Reaction-diffusion problem, (2) Diffusion-advection problem, (3) Reaction-diffusion-advection problem I and (4) Reaction-diffusion-advection problem II. All of the computations and plottings are carried by using MATLAB. We perform our experiments for various values of ε and N where ε and N are the diffusivity constant and the number of linear elements respectively. Numerical solutions are presented in terms of contours and level (surface) plots comparing with the exact solution. In the figures the maximum absolute errors are also marked. Some plots are drawn at the center line $y = 0.5$ to observe the behavior of the numerical solution compared to the exact solution.

2.2.1 Problem 1 : Reaction-diffusion problem

The reaction-diffusion problem given in [4] is obtained by taking $\mathbf{a} = (0,0)$, $b = 1$, $f = 1$ in equation (2.2). The problem is therefore

$$\begin{cases} -\varepsilon\nabla^2 u + u = 1 & \text{in} \quad 0 \le x, y \le 1 \\ u = 1 & \text{on} \quad x = 0, \quad 0 < y < 1 \\ u = 0 & \text{on} \quad x = 1, \quad 0 < y < 1 \\ \dfrac{\partial u}{\partial n} = 0 & \text{on} \quad y = 0, \quad y = 1. \end{cases} \tag{2.37}$$

The exact solution to this problem is given as [4]

$$u(x,y) = 1 - \sinh(\varepsilon^{-1/2}x)/\sinh(\varepsilon^{-1/2}). \tag{2.38}$$

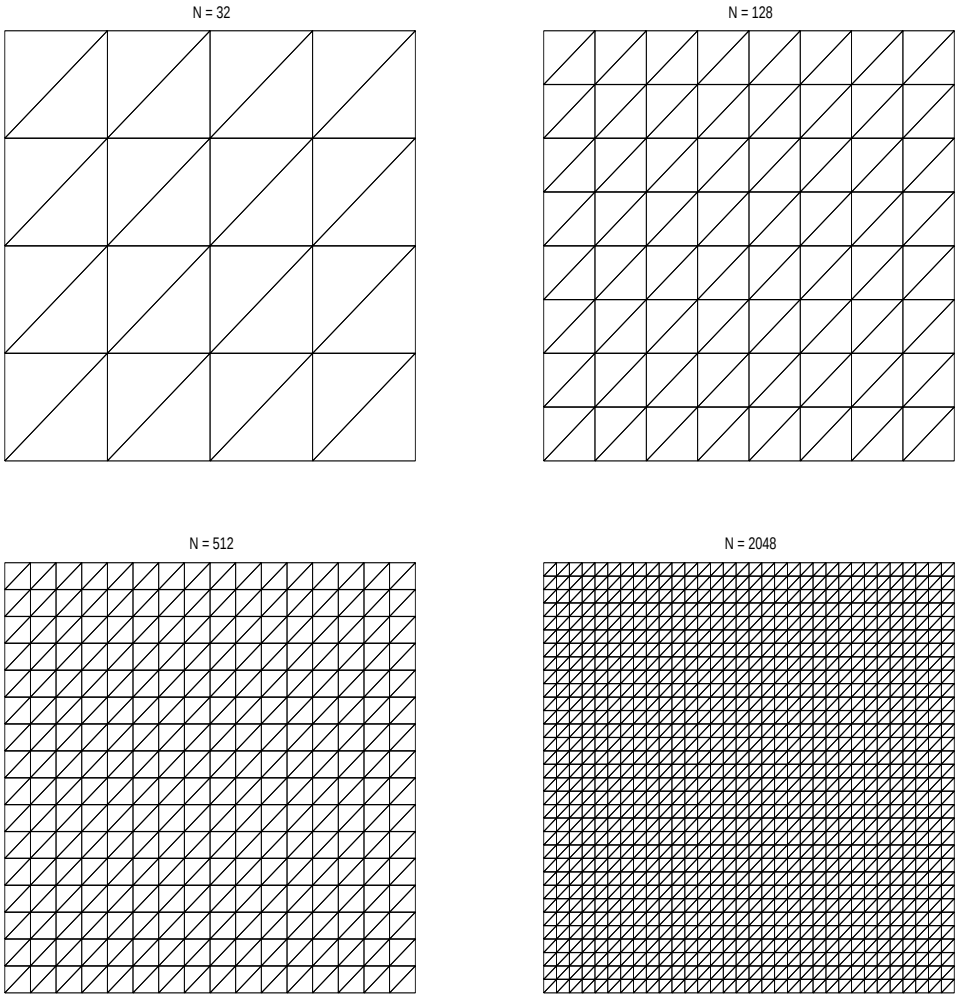

Figure 2.2: Linear triangle elements used in discretization of the problem domain

First, we take $\varepsilon = 1$, 0.1, 0.01, 0.001 and 0.0001 with N=32, 128, 512 and 2048 to observe how the diffusion effects the standard finite element solution when diffusion constant ε gets smaller. Thus, we observe that when ε gets smaller we need to take more elements in FEM.

From Figures 2.3, 2.4, 2.5 and 2.6 we can see that when ε gets smaller the standard finite element method fails to agree with the exact solution. When ε is greater than 0.001 the method provides accurate solution with increasing number of elements. However, for smaller values, although the method proves better with increasing N we see that there are still oscillations and a relatively large error occurs due to these oscillations. Therefore it is useful here to introduce the stabilized finite element method described in Section 2.1.1. Since the results obtained for ε=1, 0.1 and 0.01 are already suitable with the exact solution we will only print the plots of the stabilized method for ε=0.001 and 0.0001. For small values of ε, the contour curves accumulate along the $x = 1$ boundary of the domain and hence the contour plots does not give a sufficient

sight for observation. So, we only print the surface plots of the corresponding standard solution, the stabilized solution and the exact solution respectively to compare the standard method and the stabilized method.

As it is seen from Figures 2.7, 2.8, 2.9 and 2.10 stabilization removes the oscillations produced by the standard method. Especially when $\varepsilon = 0.0001$, the solution obtained by using the standard method is not smooth even when 2048 elements are used while the stabilization produces a smoother solution with the same number of elements.

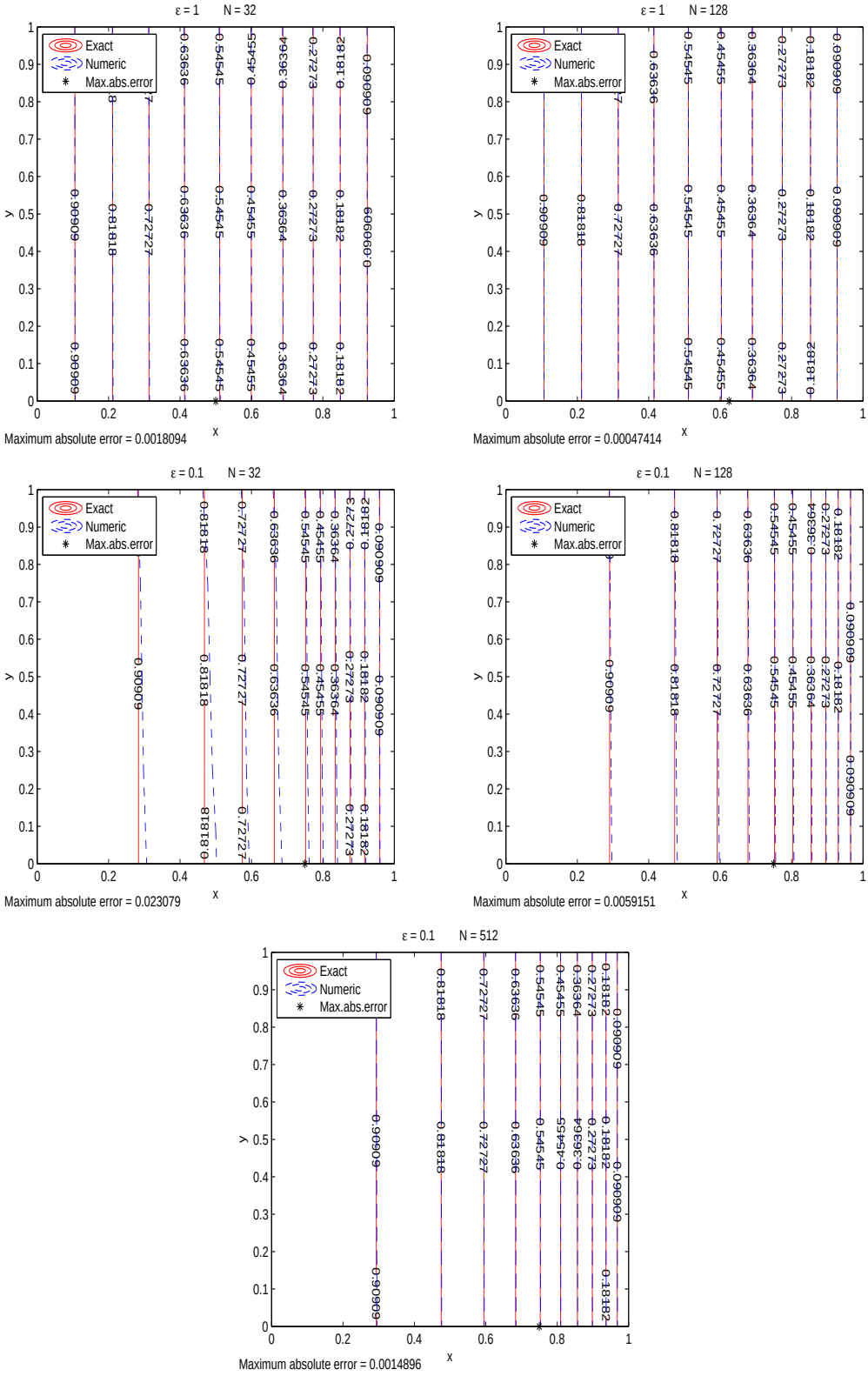

Figure 2.3: Contour plots of problem 1 for ε=1 and ε=0.1 with various values of N

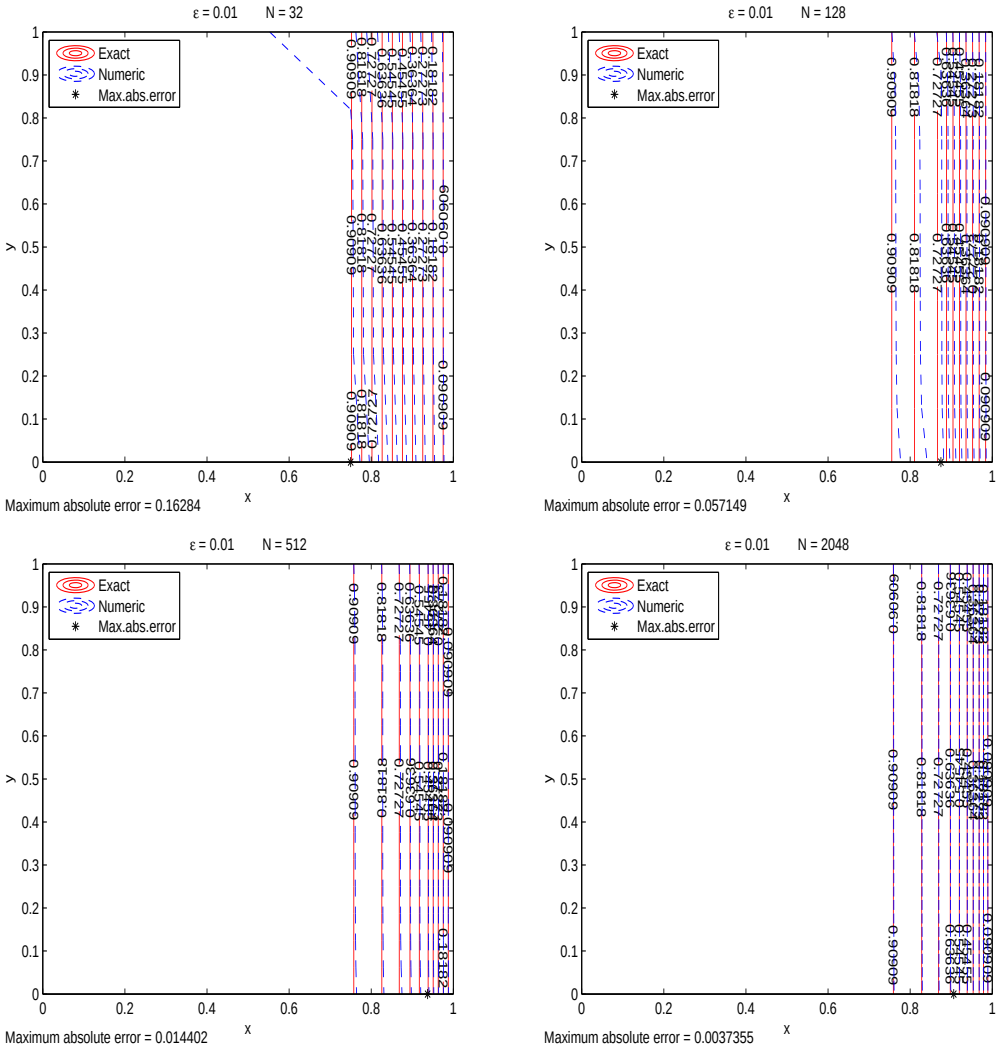

Figure 2.4: Contour plots of problem 1 for ε=0.01 with various values of N

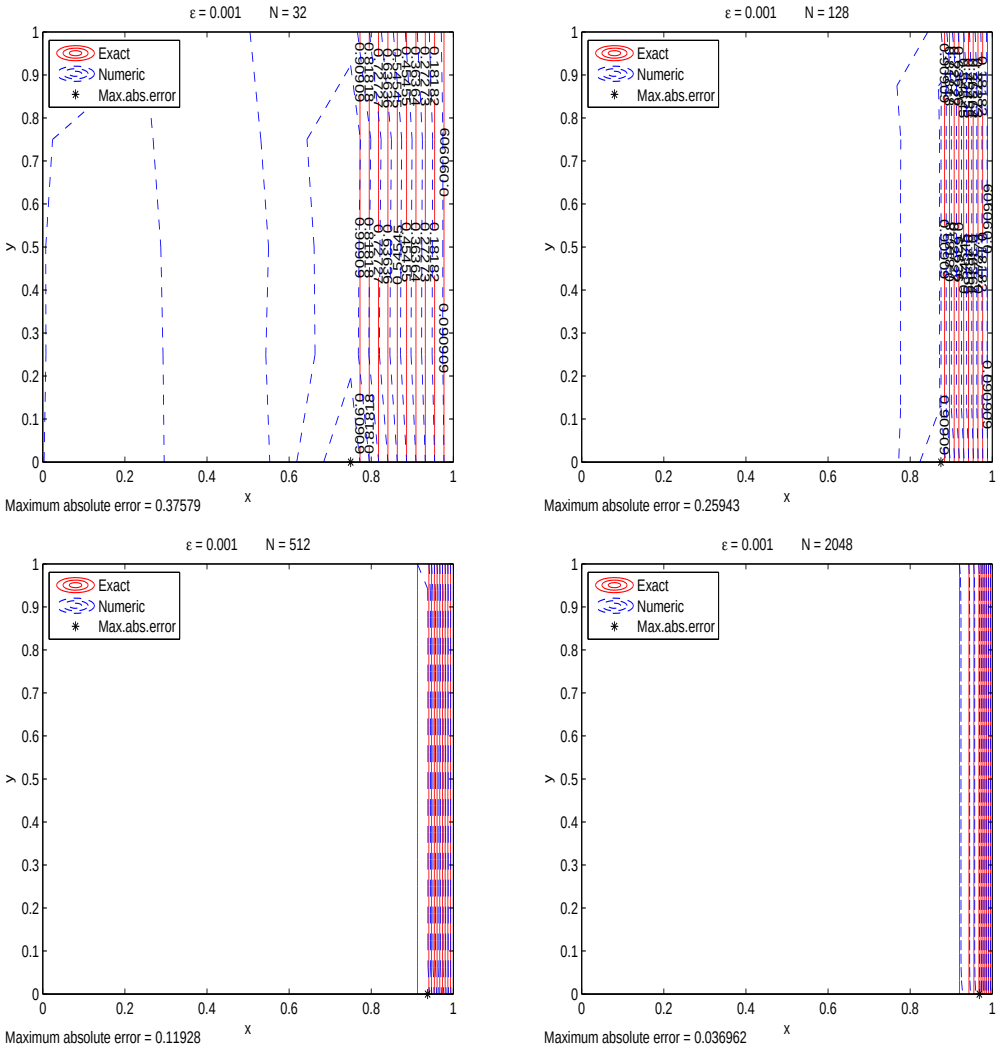

Figure 2.5: Contour plots of problem 1 for ε=0.001 with various values of N

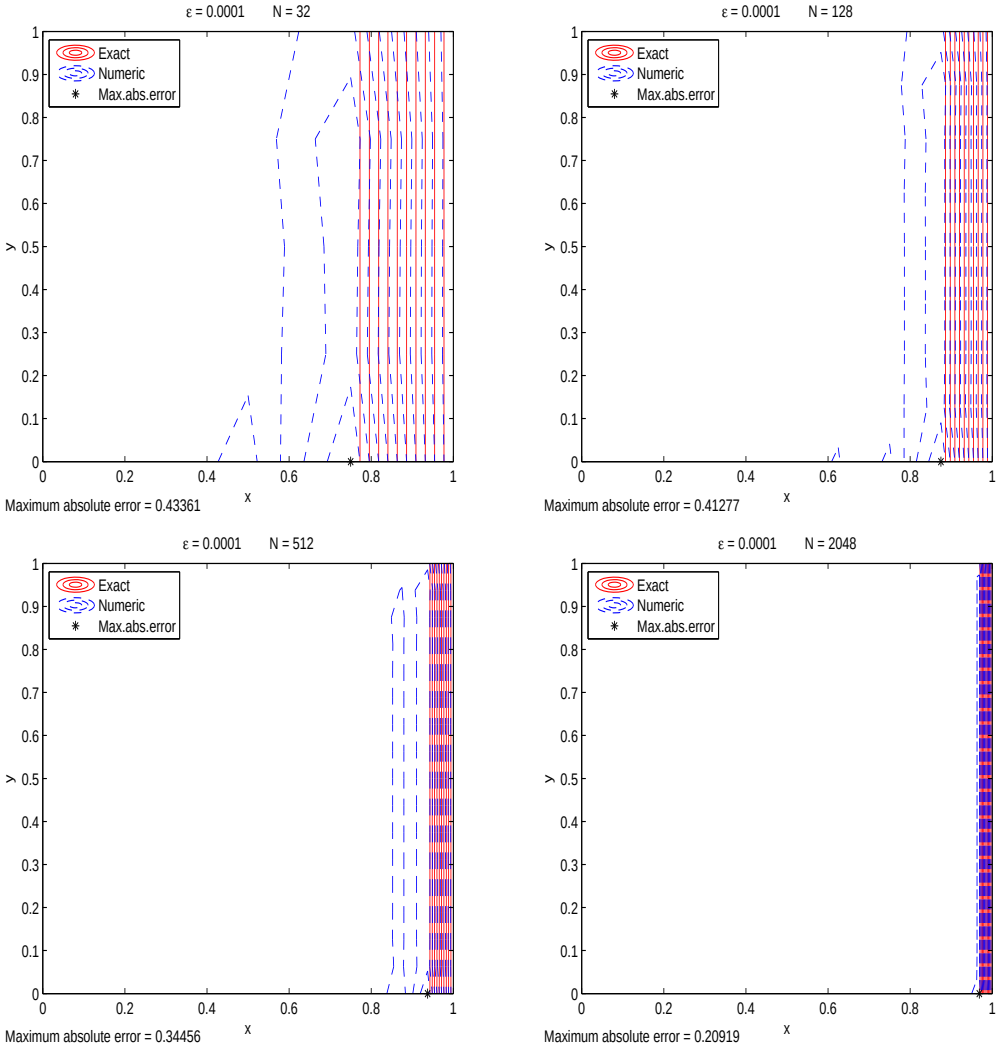

Figure 2.6: Contour plots of problem 1 for ε=0.0001 with various values of N

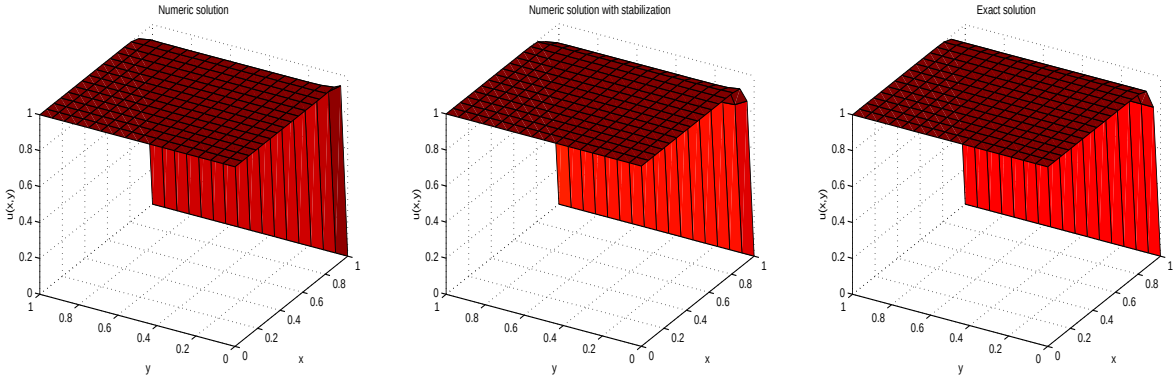

Figure 2.7: Surface plots of problem 1 for $\varepsilon = 0.001$ and N=512

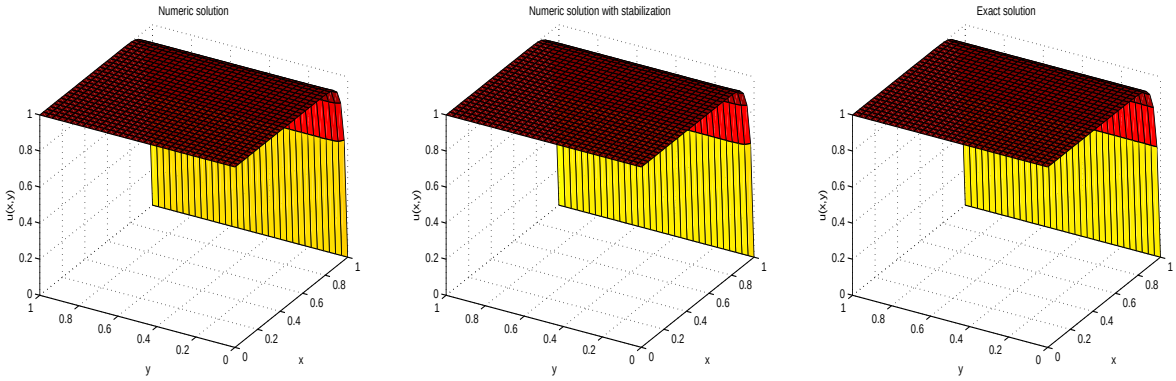

Figure 2.8: Surface plots of problem 1 for $\varepsilon = 0.001$ and N=2048

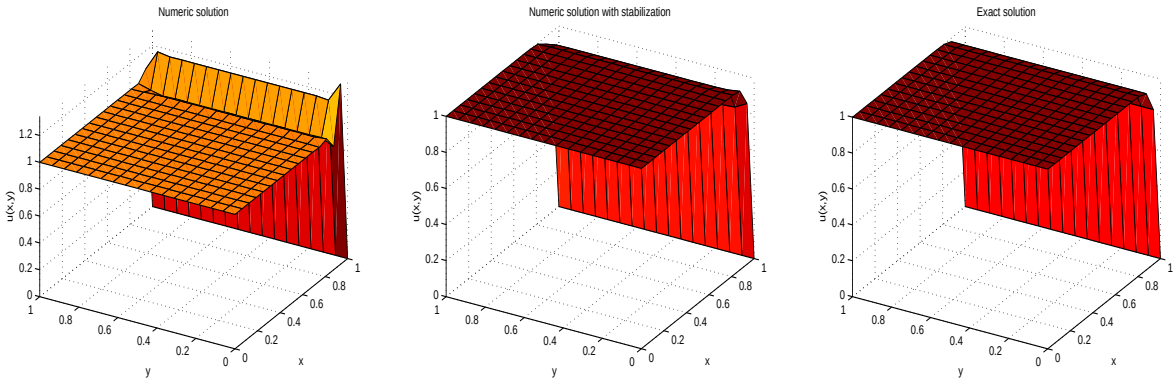

Figure 2.9: Surface plots of problem 1 for $\varepsilon = 0.0001$ and N=512

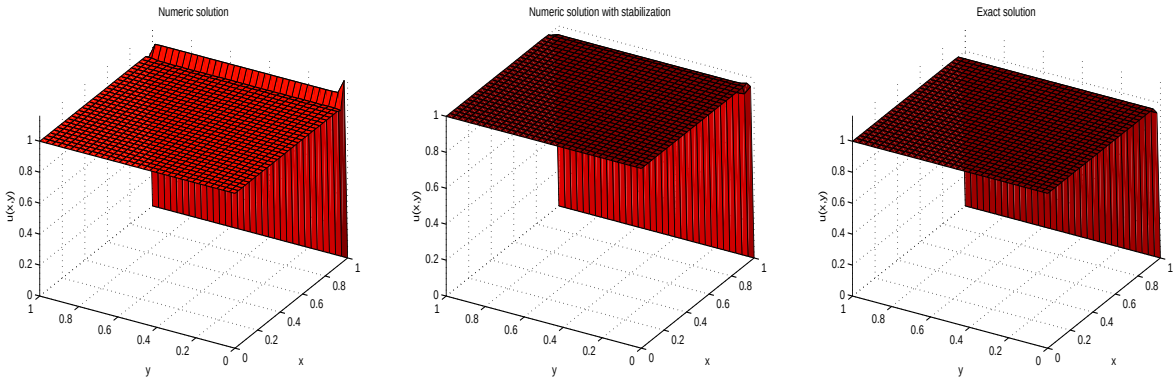

Figure 2.10: Surface plots of problem1 for $\varepsilon = 0.0001$ and N=2048

2.2.2 Problem 2 : Diffusion-advection problem

The diffusion-advection problem given in [4] is obtained by taking $\mathbf{a} = (1, 0)$, $b = 0$ and $f = 1$ in equation (2.2). The problem now turns to be

$$\begin{cases} -\varepsilon\nabla^2 u + u_x = 1 & \text{in} \quad 0 \le x, y \le 1 \\ u = 0 & \text{on} \quad x = 0, \quad x = 1, \quad 0 \le y \le 1 \\ \dfrac{\partial u}{\partial n} = 0 & \text{on} \quad y = 0, \quad y = 1, \quad 0 \le x \le 1. \end{cases} \tag{2.39}$$

The exact solution to this problem is given as [4]

$$u(x, y) = x - (e^{-\frac{1-x}{\varepsilon}} - e^{-\frac{1}{\varepsilon}})/(1 - e^{-\frac{1}{\varepsilon}}). \tag{2.40}$$

For this problem, the plots of the solutions for several values of ε and N are presented. We will test methods for $\varepsilon = 1$, 0.1, 0.01, 0.001 and 0.0001 in the given order. The existence of advection term in this problem causes a decrease in the performance of the standard method and increases the need to use stabilization. For example, when $\varepsilon = 1$ we need 512 elements to obtain a very well agreement of the numerical solution obtained with the standard method and the exact solution. This was obtained with 128 elements for problem 1 in which there was no advection. In Figure 2.11 we display the contours of the solutions for ε=1 with the standard method and the stabilized method. From these plots it can be seen that when ε is not small that is when the problem is not advection dominated, increasing number of elements increases the accuracy of the method much more than the stabilization effects. However, from Figure 2.12 it is seen that stabilization starts to prove accuracy when ε is small. The maximum error decreases and the lines are getting smoother. As before, for smaller values of ε we print the surface plots of the solutions obtained by the standard method, stabilized method and the exact solution for a better sight. Figure 2.13 shows the importance of the stabilization for $\varepsilon = 0.01$ more clearly.

From Figure 2.14 and Figure 2.15 we observe that when $\varepsilon = 0.001$ and 0.0001 the standard method fails to produce smooth solutions. Increasing number of elements does not help the solution get better. However, the stabilized method obviously removes the oscillations even with N=128. Moreover, we see that the need of the stabilization increases and the effect of increasing the number of elements decreases as ε gets smaller. For a closer look, we also display the horizontal cuts at $y = 0.5$ of the standard solution, stabilized solution and the exact solution in Figure 2.16 with N= 32, 128 and 512 for $\varepsilon = 0.0001$. From this figure as well, we can see that there is no significant oscillation in the stabilized method solution whereas the standard method solution is far away from the exact solution. Figure 2.17 shows horizontal cuts at $y = 0.5$ of the stabilized solution and the exact solution. Here again we only print the results for $\varepsilon = 0.0001$ with N=32, 128, and 512 and we see that the stabilized solution agrees well with the exact solution for small number of elements. Moreover the accuracy of the method increases as the

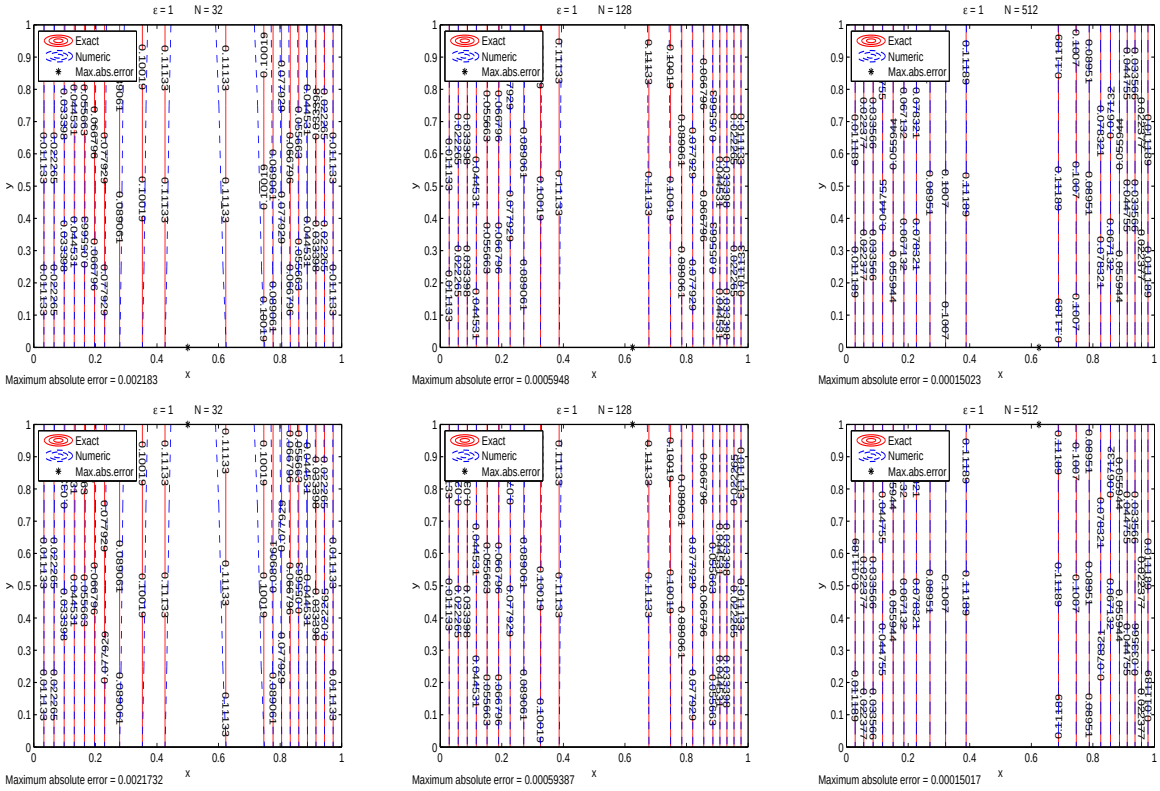

Figure 2.11: Contour plots of problem 2 with the standard method (top) and the stabilized method (bottom) for $\varepsilon = 1$ with N=32, 128 and 512

number of elements increases. Note that using 128 elements provides an accurate solution in the stabilized method.

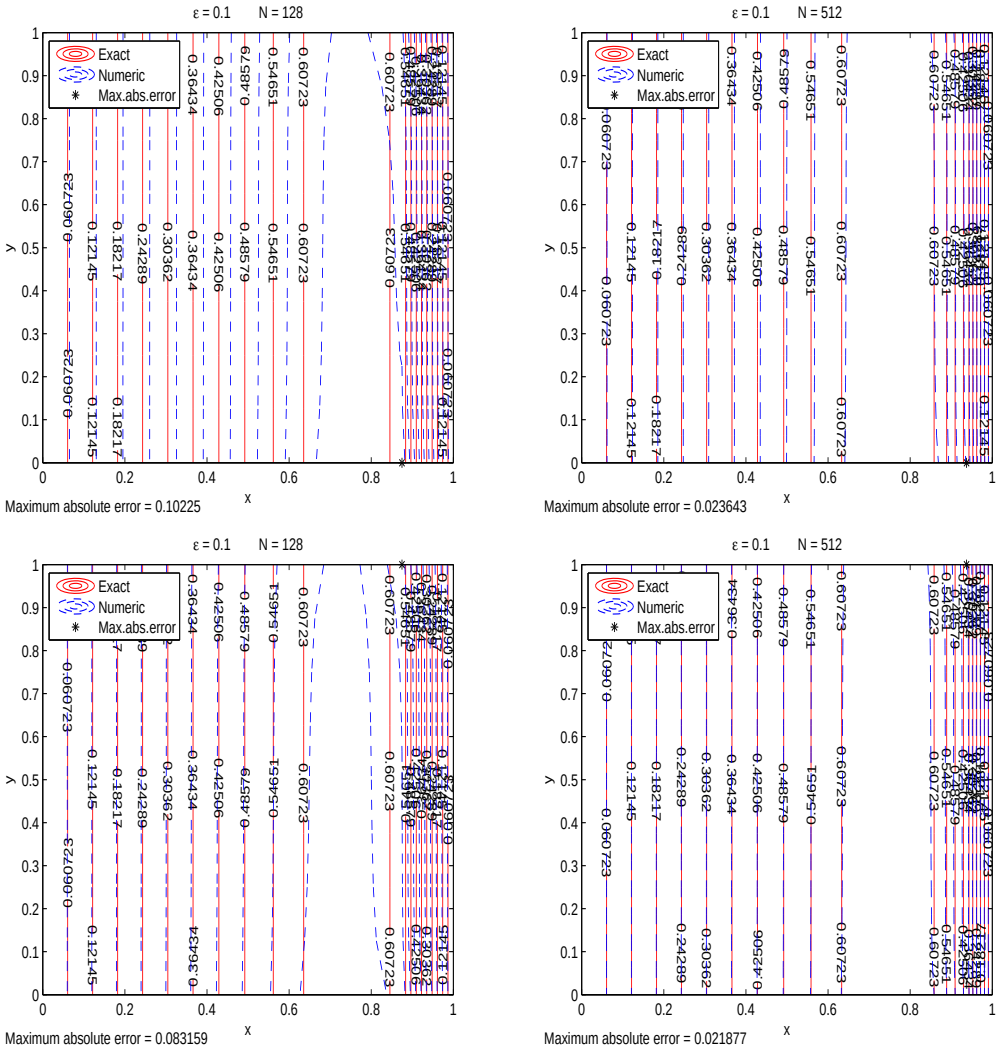

Figure 2.12: Contour plots of problem 2 with the standard method (top) and the stabilized method (bottom) for $\varepsilon = 0.1$ with N= 128 and 512

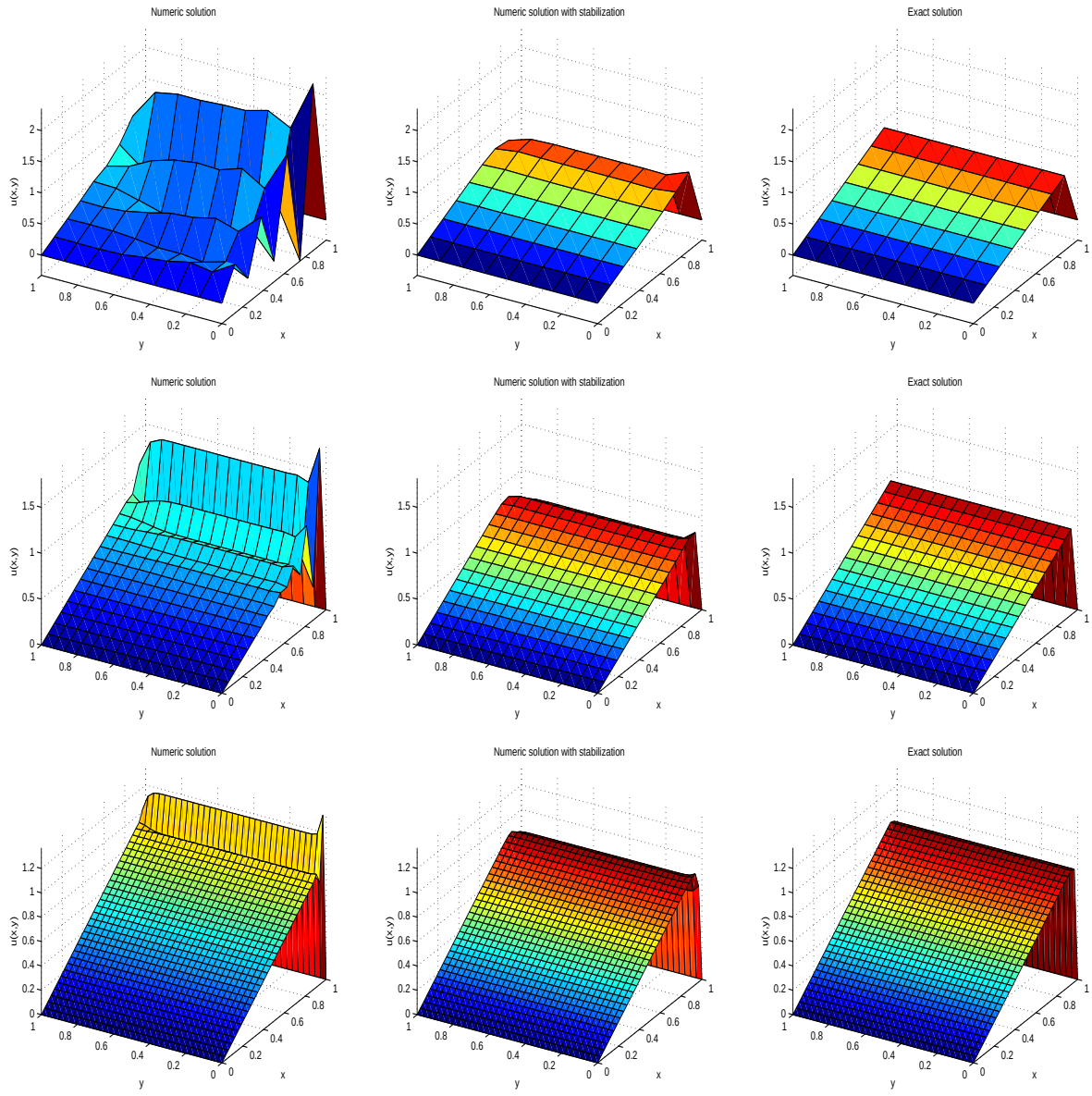

Figure 2.13: Surface plots of problem 2. The standard method, the stabilized method and the exact solution respectively for $\varepsilon = 0.01$ with N=128 (top), 512 (middle) and 2048 (bottom)

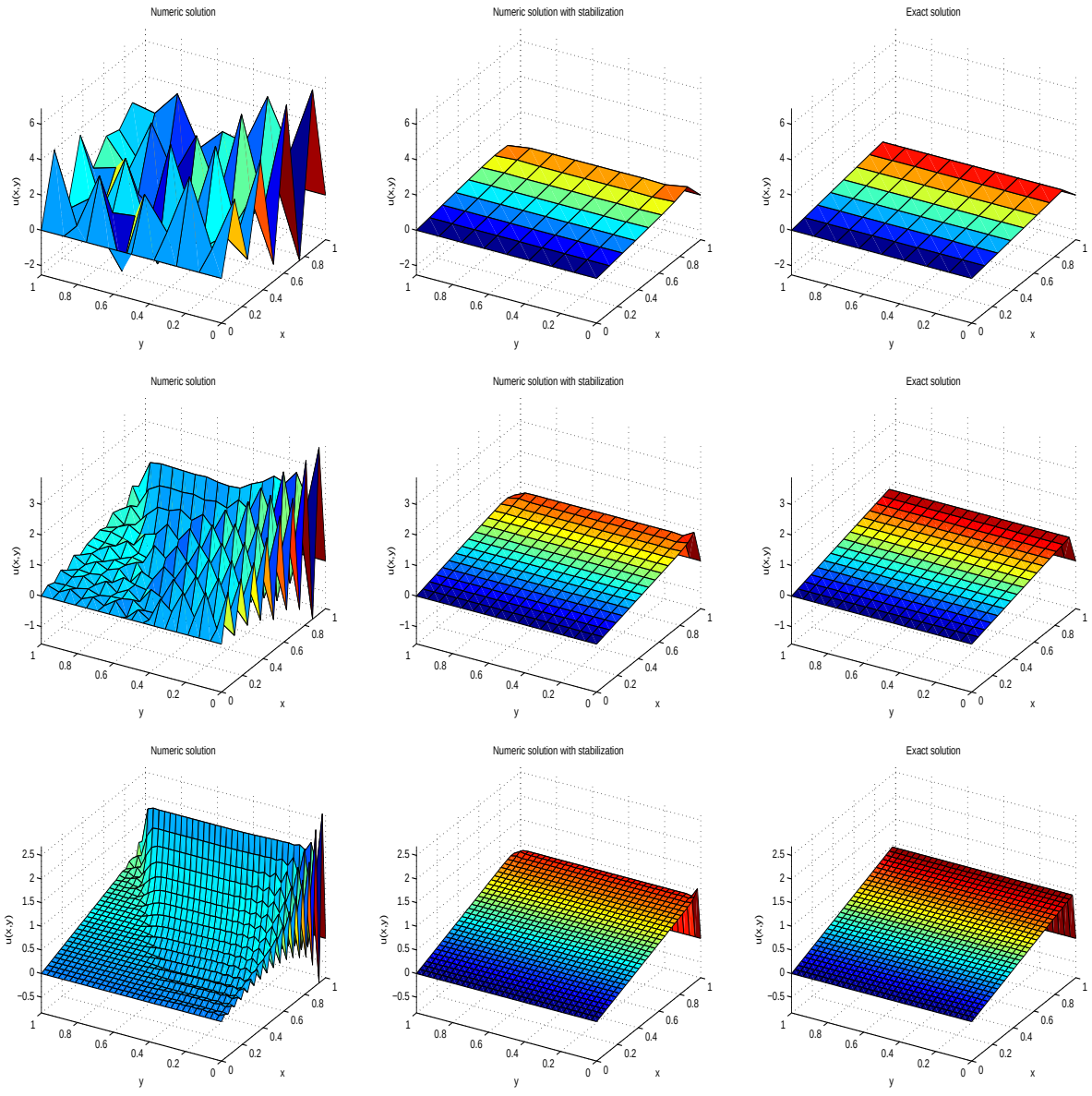

Figure 2.14: Surface plots of problem 2. The standard method, the stabilized method and the exact solution respectively for $\varepsilon = 0.001$ with N=128 (top), 512 (middle) and 2048 (bottom)

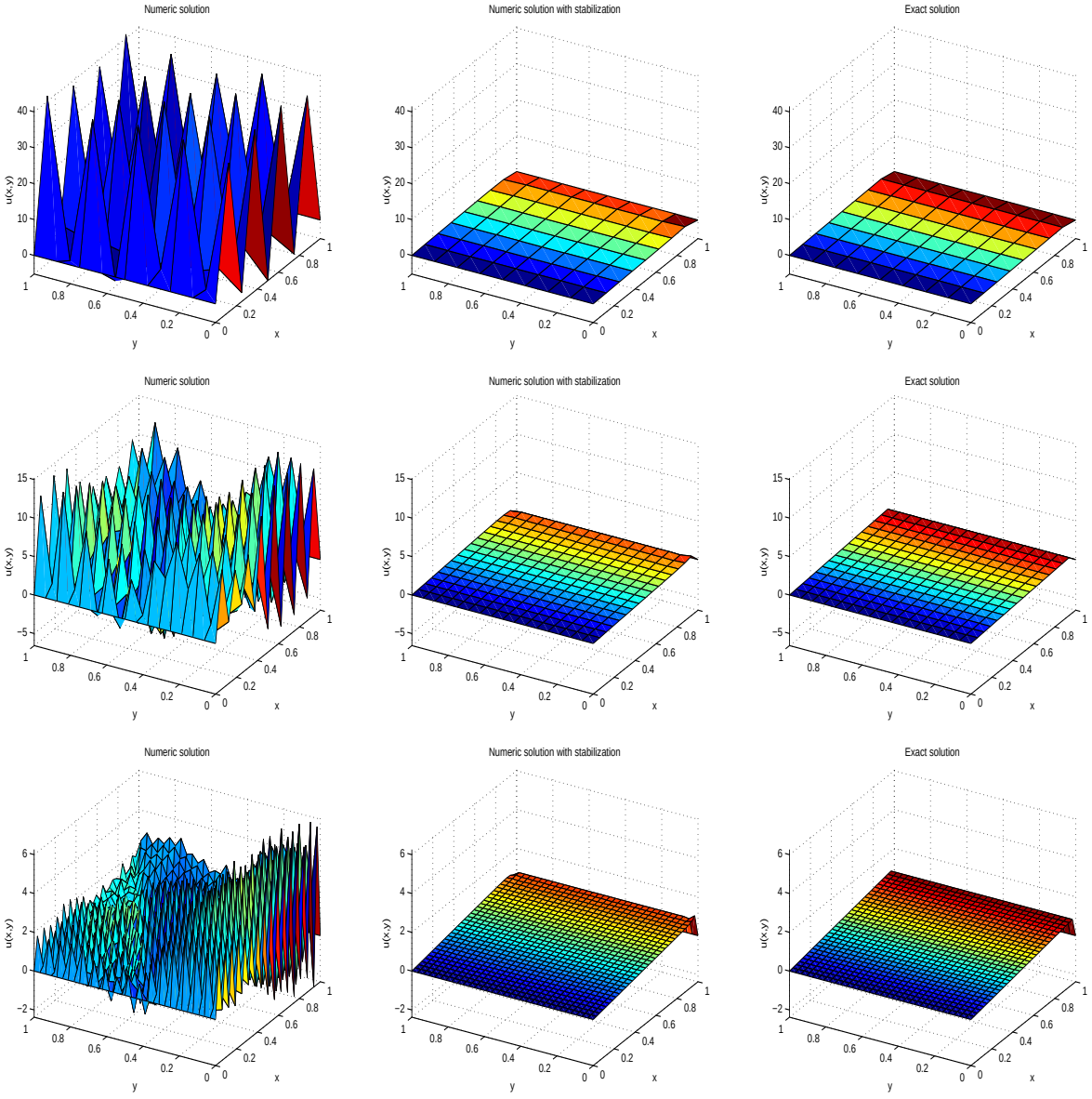

Figure 2.15: Surface plots of problem 2. The standard method, the stabilized method and the exact solution respectively for $\varepsilon = 0.0001$ with N=128 (top), 512 (middle) and 2048 (bottom)

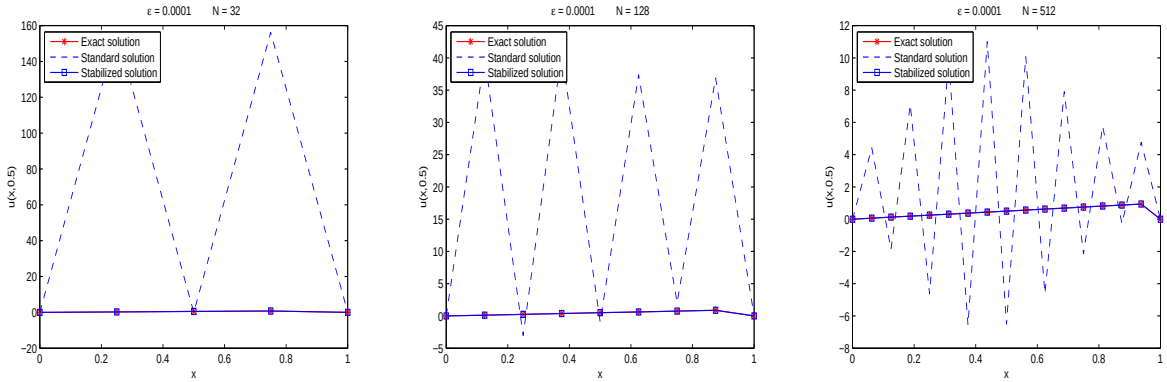

Figure 2.16: Horizontal cuts at y=0.5 of problem 2 for $\varepsilon = 0.0001$ with N=32, 128 and 512.

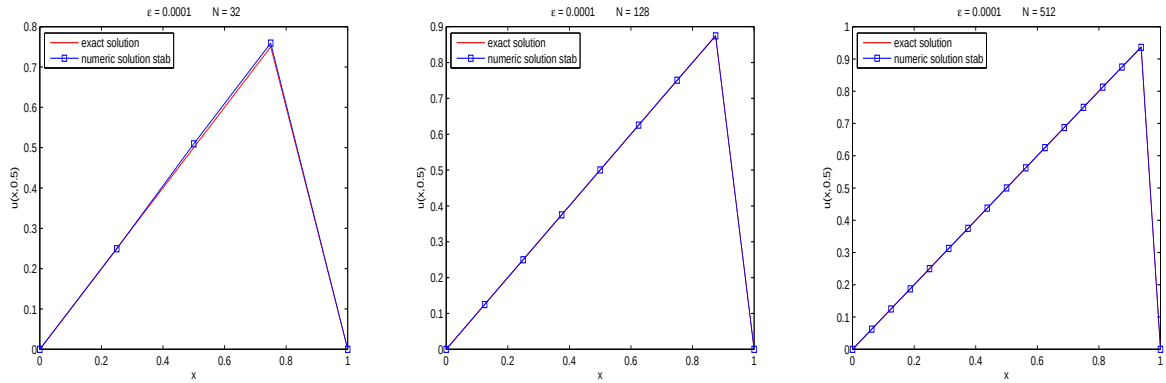

Figure 2.17: Horizontal cuts at y=0.5 of problem 2 for $\varepsilon = 0.0001$ with N=32, 128 and 512.

2.2.3 Problem 3 : Reaction-diffusion-advection problem I

Our first RDA equation is taken from [13]. In equation (2.2) we take $\varepsilon = 10^{-5}$, $\mathbf{a} = (1, 0)$ and $b = 1$. The source function f and Dirichlet boundary conditions are taken from the exact solution

$$u(x, y) = \exp(-\frac{(x - 0.5)^2}{a_w} - \frac{3(y - 0.5)^2}{a_w}) \tag{2.41}$$

with $a_w = 0.2$.

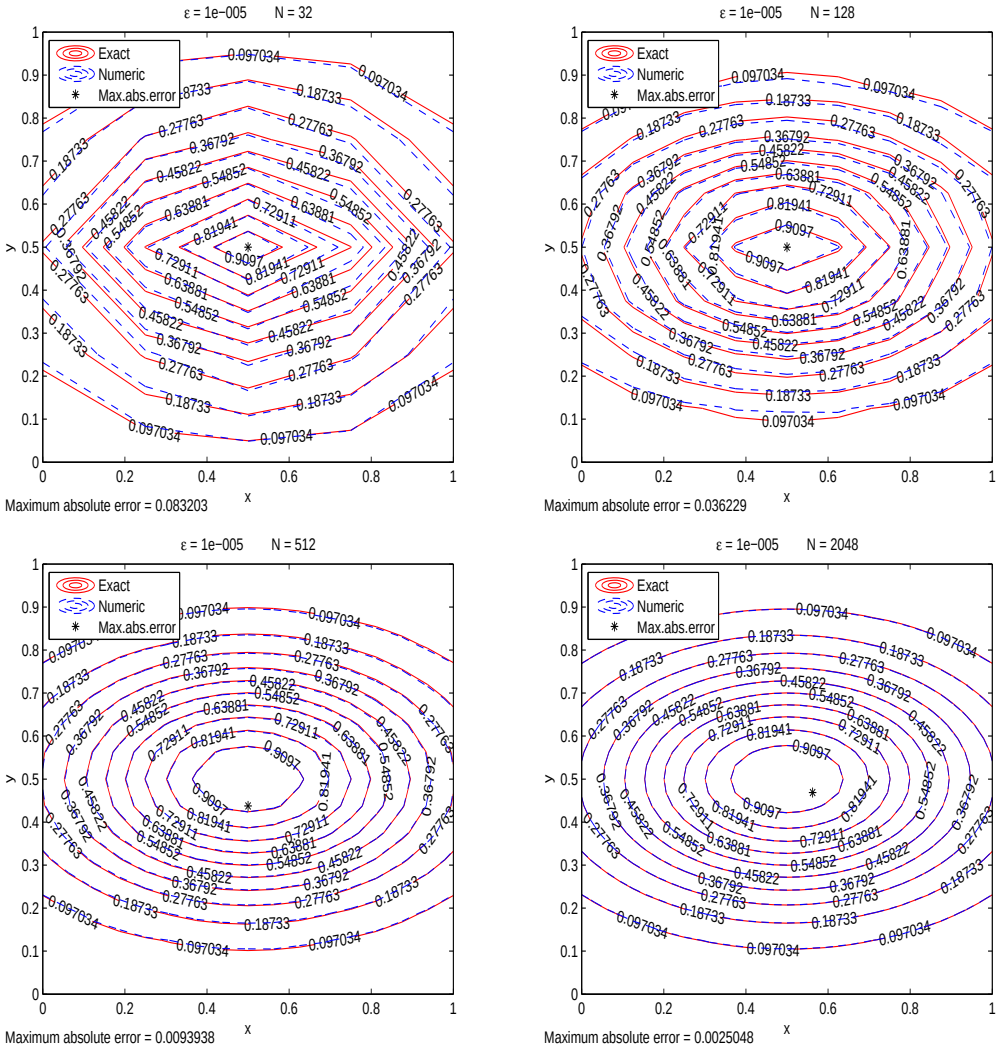

Figure 2.18: Contour plots of problem 3 for $\varepsilon = 10^{-5}$ with N=32, 128, 512 and 2048.

We solve this problem to test the reliability of the standard method to solve the RDA equations described earlier. Although the problem is advection and reaction dominated since $\varepsilon = 10^{-5}$, that is very small compared to advection and reaction paramaters, it has a smooth solution. Note that the solution does not depend on the diffusion parameter. We can see from Figure 2.18 that the solution of this problem obtained by the standard FEM agrees well with the

exact solution. Accuracy obtained increases with the increase of N as expected. The standard solution does not produce oscillations and hence, there is no need to apply the stabilized method for this problem.

2.2.4 Problem 4 : Reaction-diffusion-advection problem II

Our second steady-state RDA equation is taken from [38]. This problem is obtained by taking $\mathbf{a} = (-1, -1)$ and $b = 2$ in equation (2.2) with homogeneous Dirichlet boundary conditions. The source function f is taken to satisfy the exact solution which is given as

$$u(x, y) = (1 - e^{-x/\varepsilon})(1 - e^{-y/\varepsilon})(1 - x)(1 - y). \tag{2.42}$$

We have already tested, in the previous problem, the standard method solution for RDA equation. However, in this problem, we concentrate on the case when ε is very small and the standard solution produces oscillations unless the solution is smooth. We will consider the case $\varepsilon = 10^{-8}$, the smallest value of ε tested in [38]. To observe the behavior of the solutions we choose to plot the horizontal cuts at $y = 0.5$ again. We first show the standard solution and the exact solution for various values of N in Figure 2.19. We see that for this problem the standard FEM fails to produce a reasonable solution even when $N = 2048$. Hence, the need for stabilization is obvious. The next plot, Figure 2.20 shows the standard FEM solution, the stabilized method solution and the exact solution along $y = 0.5$ to be able to compare the methods. It can be seen from the figure that the stabilized method reveals the oscillations produced by the standard FEM. Hence, the reaction-advection dominated RDA equation is solved properly for $\varepsilon = 10^{-8}$ by using 2048 elements.

These test problems show that as ε gets smaller the standard FEM needs more elements to obtain accurate solution. For smaller values of ε however, increasing the number of elements does not reveal the nonphysical oscillations in the standard FEM solution and in this case the stabilized FEM is used. The stabilized FEM produces more accurate solutions with less number of elements compared to standard Galerkin FEM. Moreover, it avoids those nonphysical oscillations.

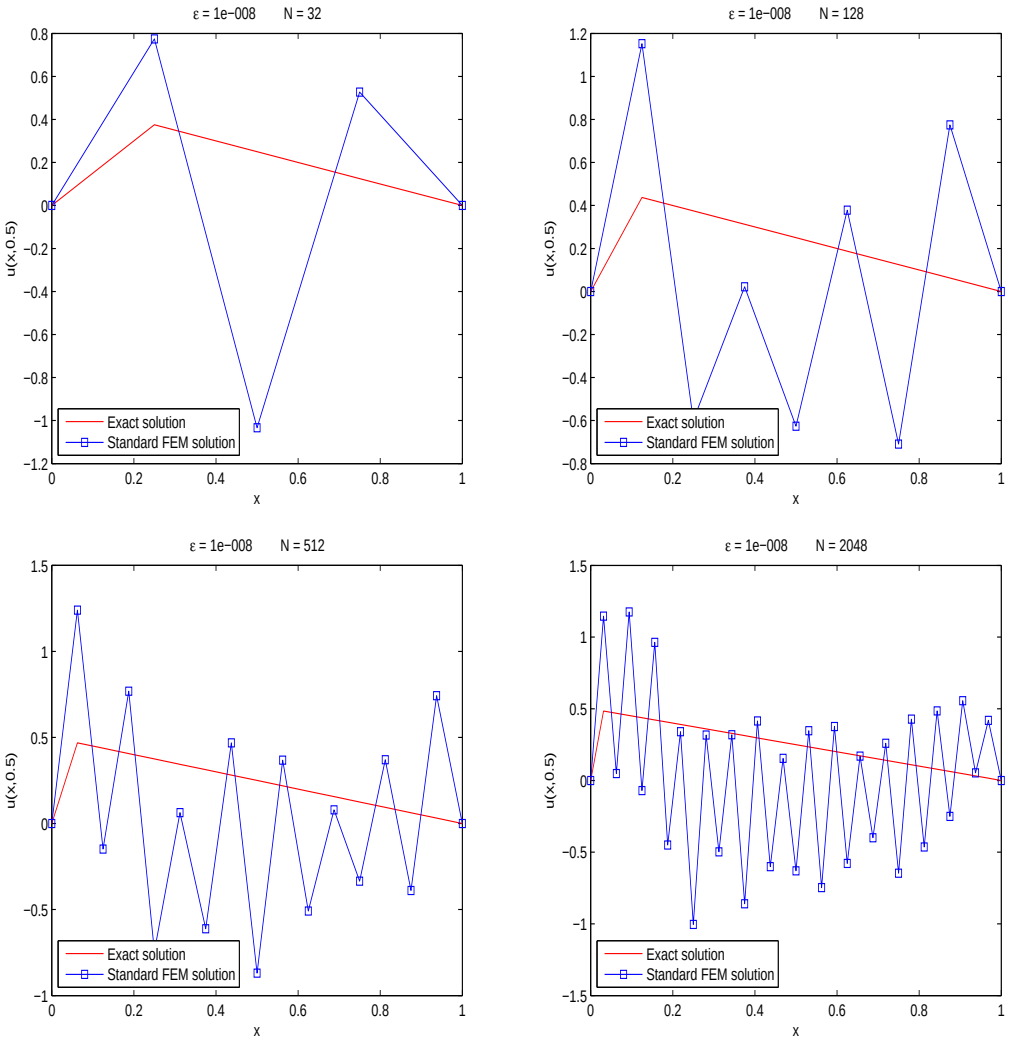

Figure 2.19: Horizontal cuts of the standard method solution and the exact solution of problem 4 at $y = 0.5$ with N=32, 128, 512 and 2048.

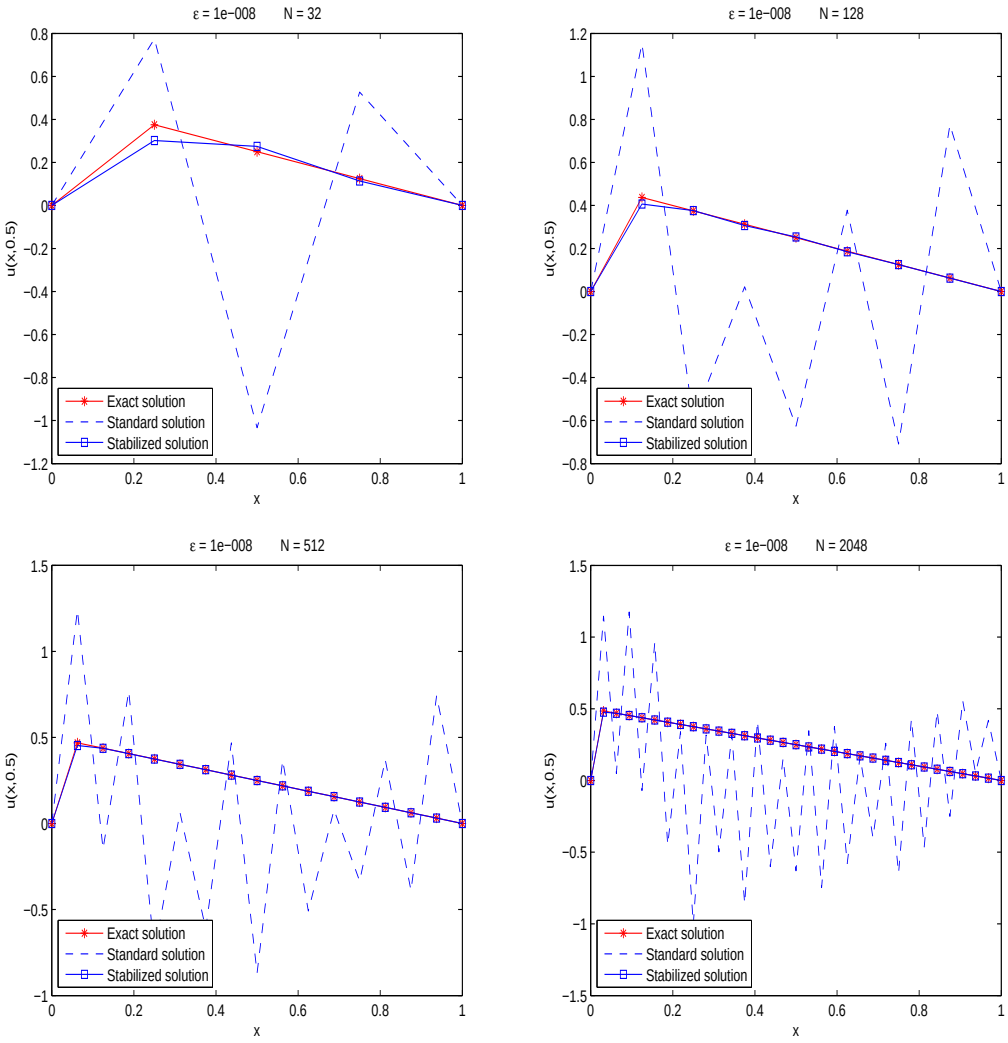

Figure 2.20: Horizontal cuts of the standard method solution, stabilized method solution and the exact solution of problem 4 at $y = 0.5$ for N=32, 128, 512 and 2048.

Chapter 3

Finite Element Method Solution of Time-Dependent Reaction-Diffusion-Advection Equations

In this chapter, we describe the FEM analysis for time-dependent RDA equations using a two-dimensional model problem. The finite element model for time-dependent problems involves two main steps. The first step, called semidiscretization, is to obtain the weak form of the equation on an element to find the spatial approximation. As a result of the semidiscretization a set of ordinary differential equations in time with nodal values is obtained. The second step is the time approximation of these ordinary differential equations. Using a finite difference scheme, the set of differential equations is transformed into a set of algebraic equations involving the nodal values at the time level t_{k+1} in terms of known values from the previous time level t_k. The time discretization can be done using Runge-Kutta method, least squares method, finite difference method or finite element method for time direction, details can be found in [43, 19, 6]. In this study, we use the generalized trapezoidal rule, also called as $\alpha - family$ approximation, which is described within the next section.

3.1 Finite Element Method in Space, Finite Difference Method in Time

Consider the non-dimensional time-dependent RDA equation given together with boundary conditions and initial condition

$$\begin{cases} \dfrac{\partial u}{\partial t} - \varepsilon \nabla^2 u + \mathbf{a} \cdot \nabla u + bu = f & \text{in } \Omega \times [0, T] \\ u(\mathbf{x}, t) = u_D & \text{on } \Gamma_D \\ \dfrac{\partial u}{\partial n} = q_N = g & \text{on } \Gamma_N \\ u(\mathbf{x}, 0) = u_0 & \text{at } t = 0 \end{cases} \tag{3.1}$$

where Γ_D and Γ_N are the boundaries on which the Dirichlet (or first type) boundary condition and the Neumann (or second type) boundary condition defined respectively, with $\Gamma_D \cup \Gamma_N = \partial\Omega$. In the two-dimensional case, $\mathbf{x} = (x, y)$ and hence, the boundary conditions are $u(x, y, t) = u_D(x, y, t)$, $q_N = \varepsilon \frac{\partial u}{\partial x} n_x + \varepsilon \frac{\partial u}{\partial y} n_y = g(x, y, t)$, and similarly the initial condition is $u(x, y, 0) = u_0(x, y)$. The source function f in this case is of the form $f = f(x, y, t)$.

The weak form of (3.1) over an element Ω_e can be obtained by a similar procedure used in Section 2.1. Multiply the differential equation in (3.1) with the weight function $w(x, y)$ (which is a function of position only) and integrate over the element to obtain

$$\int_{\Omega_e} w(\frac{\partial u}{\partial t} - \varepsilon \nabla^2 u + \mathbf{a} \cdot \nabla u + bu - f) dx dy = 0. \tag{3.2}$$

Then we integrate by parts with respect to position variables only using the divergence theorem. Replacing the coefficient of w in the boundary integral with the secondary variable using $q_N = \varepsilon \frac{\partial u}{\partial x} n_x + \varepsilon \frac{\partial u}{\partial y} n_y$ we obtain

$$\int_{\Omega_e} [w(\frac{\partial u}{\partial t} + a_1 \frac{\partial u}{\partial x} + a_2 \frac{\partial u}{\partial y} + bu - f) + \varepsilon \frac{\partial w}{\partial x} \frac{\partial u}{\partial x} + \varepsilon \frac{\partial w}{\partial y} \frac{\partial u}{\partial y}] dx dy - \oint_{\Gamma_e} w q_n ds = 0. \tag{3.3}$$

Now, to obtain the semidiscrete finite element model we substitute a finite model approximation for u. To select an approximation for u we assume that the time dependence and space variation can be separated, that is, we use the approximation

$$u(x, y, t) \approx \sum_{j=1}^{n} u_j^e(t) \psi_j^e(x, y) \tag{3.4}$$

where u_j^e are the values of $u(x, y, t)$ at the spatial location (x_j, y_j) at time t and n is the number of nodes of element 'e'. We now, substitute $w = \psi_i^e(x, y)$ and replace u in equation (3.3) by (3.4) to obtain the ith differential equation in time

$$\sum_{j=1}^{n} \left(M_{ij}^e \frac{du_j^e}{dt} + K_{ij}^e u_j^e \right) - f_i^e - Q_i^e = 0 \qquad i = 1, 2, ..., n \tag{3.5}$$

where

$$
\begin{aligned}
M_{ij}^e &= \int_{\Omega_e} \psi_i^e \psi_j^e dxdy \\
K_{ij}^e &= \int_{\Omega_e} \left\{ \varepsilon \left(\frac{\partial \psi_i^e}{\partial x}\frac{\partial \psi_j^e}{\partial x} + \frac{\partial \psi_i^e}{\partial y}\frac{\partial \psi_j^e}{\partial y} \right) + a_1 \psi_i^e \frac{\partial \psi_j^e}{\partial x} + a_2 \psi_i^e \frac{\partial \psi_j^e}{\partial y} + b\psi_i^e \psi_j^e \right\} dxdy \\
f_i^e &= \int_{\Omega_e} f(x,y,t)\psi_i^e dxdy \\
Q_i^e &= \oint_{\Gamma_e} \psi_i^e q_n ds.
\end{aligned}
\tag{3.6}
$$

The equation (3.5) can be written in matrix form as

$$
[M^e]\{\dot{u}^e\} + [K^e]\{u^e\} = \{f^e\} + \{Q^e\} \tag{3.7}
$$

where $\dot{u} = \dfrac{\partial u}{\partial t}$.

After the assembly procedure the system

$$
[M]\{\dot{u}\} + [K]\{u\} = \{f\} + \{Q\} \tag{3.8}
$$

is obtained, where the matrices are of sizes $n \times n$.

We should note, once again, that we used linear triangular elements in this study and therefore the matrices in (3.6) can be computed exactly using the formulas given in Section 2.1. This completes the semidiscretization step. We now describe the $\alpha - family$ approximation, in which a weighted average of the time derivative of the dependent variable is approximated at two consecutive time steps by linear interpolation of the values of the variable at the two steps

$$
(1-\alpha)\{\dot{u}\}_s + \alpha\{\dot{u}\}_{s+1} = \frac{\{u\}_{s+1} - \{u\}_s}{\Delta t_{s+1}} \qquad \text{for} \quad \alpha \in [0,1]. \tag{3.9}
$$

The $\alpha - family$ approximation is [43]

$$
\{u\}_{k+1} = \{u\}_k + \Delta t\left[(1-\alpha)\{\dot{u}\}_k + \alpha\{\dot{u}\}_{k+1}\right]. \tag{3.10}
$$

For different values of $\alpha \in [0,1]$ we obtain the following approximation schemes

$$
\alpha = \begin{cases} 0, & \text{the forward difference scheme} \\ 1/2, & \text{the Crank-Nicolson scheme} \\ 2/3, & \text{the Galerkin scheme} \\ 1, & \text{the backward difference scheme.} \end{cases} \tag{3.11}
$$

Among these, the Crank-Nicolson scheme, the Galerkin scheme and the backward difference scheme are unconditionally stable. However, the forward difference scheme is conditionally stable and the stability requirement is

$$\Delta t < \Delta t_{cr} = \frac{2}{(1-2\alpha)\,\lambda_{max}} \tag{3.12}$$

where $\alpha < \frac{1}{2}$ and λ_{max} is the largest eigenvalue of the finite element equations

$$(-\lambda\,[M^e] + [K^e])\,\{u^e\}=\{Q^e\}\,. \tag{3.13}$$

Details can be found also in [43].

Using the approximation (3.10) we transform the differential equations (3.8) into a set of algebraic equations at time t_{k+1}

$$[\hat{K}]_{k+1}\{u\}_{k+1} = \{\hat{F}\} \tag{3.14}$$

where

$$[\hat{K}]_{k+1} = [M] + \alpha\Delta t\,[K]_{k+1} \tag{3.15}$$

and

$$\{\hat{F}\} = \Delta t\left(\alpha\,\{F\}_{k+1} + (1-\alpha)\,\{F\}_k\right) + \left([M] - (1-\alpha)\,\Delta t\,[K]_k\right)\{u\}_k\,. \tag{3.16}$$

Finally, equation (3.14) is solved for the nodal values u_j at time $t_{k+1} = \Delta t(k+1)$. Note that $\{F\}$ is the sum of the source vector $\{f\}$ and internal flux vector $\{Q\}$ which are known for both time levels t_k and t_{k+1} at all nodes where we seek a solution because f is a known function and the sum of Q_j^e is zero at these nodes. Therefore, at time $t = 0$, $\{\hat{F}\}$ can be computed using the initial value of u (that is u_0). Then the solution can be obtained iteratively for any time level from equation 3.14.

3.1.1 The Stabilized finite element method for transient problems

The stabilized method for steady problems was given in Section 2.1.1. The extension to the transient problems is based on a previous discretization in time of the equation (3.1) and adding stabilizing terms to equation (3.14). The method, in each discrete time, on each element has now the form [19, 35]

$$
\begin{aligned}
&(u_k, w) + \sum \tau_K (u_k, \mathbf{a} \cdot \nabla w) + \\
&\alpha \Delta t \left[(\varepsilon \nabla u_k, \nabla w) + (\mathbf{a} \cdot \nabla u_k + b u_k, w) + \sum \tau_K (\mathbf{a} \cdot \nabla u_k + b u_k, \mathbf{a} \cdot \nabla w) \right] = \\
&(u_{k-1}, w) + \sum \tau_K (u_{k-1}, \mathbf{a} \cdot \nabla w) - \\
&\alpha \Delta t \left[(\varepsilon \nabla u_{k-1}, \nabla w) + (\mathbf{a} \cdot \nabla u_k + b u_{k-1}, w) + \sum \tau_K (\mathbf{a} \cdot \nabla u_{k-1} + b u_{k-1}, \mathbf{a} \cdot \nabla w) \right] + \\
&\alpha \Delta t \left[(f_{k-1}, w) + \sum \tau_K (f_{k-1}, \mathbf{a} \cdot \nabla w) + (f_k, w) + \sum \tau_K (f_k, \mathbf{a} \cdot \nabla w) \right]
\end{aligned}
\tag{3.17}
$$

where $(\cdot, \cdot)$ denotes the usual inner product, τ_K is the stabilization parameter defined in (2.33) and α =0.5 (Crank-Nicolson scheme) is used in the computations.

3.2 Numerical Results

In this section we present the solutions of time dependent problems. We use the unconditionally stable Crank-Nicolson scheme ($\alpha = 0.5$ in equation (3.10)) for the temporal discretization with different Δt and different N values. Several values of Δt and N are tested to find the best solution in each test problem. The problems we solve are (1) Heat conduction problem, (2) Diffusion problem, (3) Reaction-diffusion problem, (4) Diffusion-advection problem, (5) System of reaction-diffusion equations , (6) Reaction-diffusion system (7) Reaction-diffusion Brusselator system, (8) Reaction-diffusion-advection problem and (9) A basic air pollution model.

3.2.1 Problem 1 : Heat conduction problem

We first consider the transient heat conduction equation from [43]

$$
\frac{\partial u}{\partial t} - \nabla^2 u = 1 \qquad \text{on } \Omega \times [0, T] \tag{3.18}
$$

where $\Omega = [0, 1] \times [0, 1]$ with initial condition

$$
u(x, y, 0) = 0 \qquad \text{for all (x,y) in } \Omega \tag{3.19}
$$

and subject to the boundary conditions,

$$
\begin{aligned}
&u(1, y, t) = u(x, 1, t) = 0 \text{ and} \\
&\frac{\partial u}{\partial x}(0, y, t) = \frac{\partial u}{\partial y}(x, 0, t) = 0.
\end{aligned}
\tag{3.20}
$$

The exact solution is not given explicitly to this problem. However, it is reported that the steady state is reached at $t = 1$ and some of the nodal values of the exact solution at $t = 1$ are listed in [43]. For experiments we pick the middle node, $(0.5, 0.5)$, of the the problem domain to compare the given exact value and the computed value using finite element method. It is known that $u(0.5, 0.5, 1) = 0.1811$. We take $N = 32$ and test the method for several Δt values and the results are given in Table 3.1.

Table 3.1: Maximum absolute errors of problem 1 for several Δt values with $N = 32$

Δt	u(0.5,0.5,1)	Maximum absolute error
0.1	0.1794	0.0017
0.05	0.1791	0.0020
0.01	0.1790	0.0021
0.001	0.1790	0.0021

The table shows that the unconditionally stable scheme produces close results but $\Delta t = 0.1$ obtains the smallest error. Hence, we use $\Delta t = 0.1$ for the following computations. Next we take $\Delta t = 0.1$ and now seek the steady state solution using several number of elements. To find the steady state solution to this problem we terminate when $|u_k - u_{k-1}|$ is less then a given *tolerance*. We set the *tolerance* to 10^{-4} and obtained the results in Table 3.2.

Table 3.2: Maximum absolute errors of problem 1 for several N values with $\Delta t = 0.1$

N	FEM solution	Reached time	Maximum absolute error
32	0.1794	1.1	0.0017
128	0.1804	1.2	6.8846e-004
512	0.1809	1.4	2.0581e-004
2048	0.1810	1.4	1.4980e-004

We can see from Table 3.2 that the steady solution at the middle node is already obtained for $\Delta t = 0.1$ with $N = 128$. Now, we can proceed to have a look at the solution on the whole domain. We plot the contours of the steady solution in Figure 3.1. We see from the plot that the finite element solution is consistent with the boundary conditions. The solution vanishes along the $x = 1$ and $y = 1$ boundaries and level curves are perpendicular to the boundaries $x = 0$ and $y = 0$ and this validates the given homogenous Neumann boundary conditions of the problem.

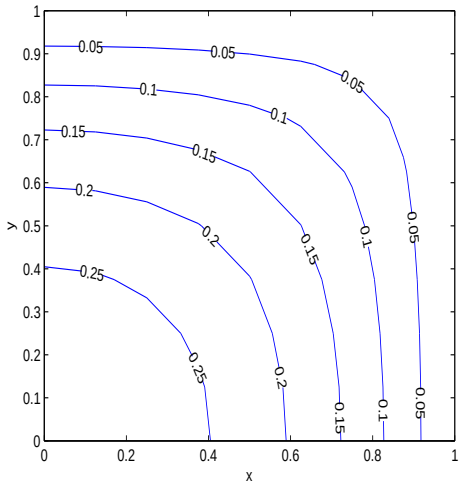

Figure 3.1: Contour plot of problem 1 at steady state with $\Delta t = 0.1$ and N=128

3.2.2 Problem 2 : Diffusion problem

We consider the time dependent linear diffusion equation from [17]. The problem is

$$\frac{\partial u}{\partial t} - \nabla^2 u = 0 \qquad \text{on } \Omega \times [0, T] \tag{3.21}$$

where $\Omega = [0, 1] \times [0, 1]$ with initial condition

$$u(x, y, 0) = \sin(\pi x) \sin(2\pi y) \tag{3.22}$$

and the Dirichlet boundary conditions are

$$u(0, y, t) = u(1, y, t) = u(x, 0, t) = u(x, 1, t) = 0. \tag{3.23}$$

The exact solution to this problem is given as [17]

$$u(x, y, t) = e^{-5\pi^2 t} \sin(\pi x) \sin(2\pi y). \tag{3.24}$$

Figure 3.2 shows the exact solution at the point $(0.5, 0.5)$ that is $u(0.5, 0.5)$ in the time interval $t = [0, 1]$. We see that the exact solution to this problem goes to zero after a short time. To compare the exact solution and the FEM solution we print the results for $t = 0.05$ in Figure 3.3. These results show that for solving the transient diffusion problem, $N = 32$ and $N = 128$ are not enough, however, when $N = 512$ the solution agrees well with the exact solution and the best accuracy is obtained when $N = 2048$.

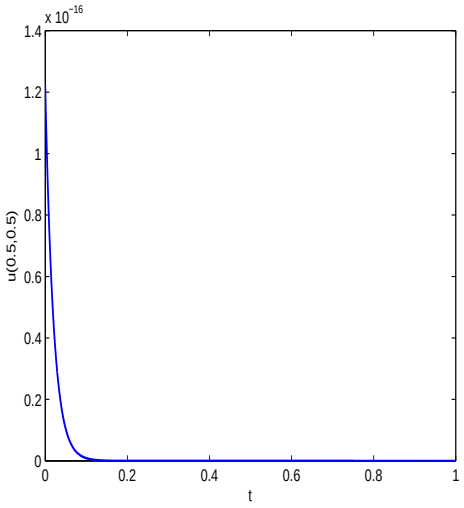

Figure 3.2: Plot of exact solution of problem 2 at (0.5,0.5)

3.2.3 Problem 3 : Reaction-diffusion problem

We consider now the nonlinear reaction-diffusion equation

$$\frac{\partial u}{\partial t} - \frac{1}{2}\left(\frac{\partial^2 u}{\partial x^2} + \frac{\partial^2 u}{\partial y^2}\right) = u^2\,(1-u) \qquad \text{in } \Omega \times [0,T] \tag{3.25}$$

where $\Omega = [0,1] \times [0,1]$ and Dirichlet boundary conditions together with the initial condition are taken to be consistent with the exact solution which is given in [17] as

$$u(x,y,t) = \frac{1}{1+e^{p(x+y-pt)}} \qquad \text{where } p = \frac{1}{\sqrt{2}}. \tag{3.26}$$

For this problem, we first fix $N = 32$ to experiment the best value for Δt. We take Δt= 0.1, 0.01, 0.001 and 0.0001 to reach the time level $t = 1$ and compare by looking at the maximum error between the calculated solution and the exact solution. The results are listed in Table 3.3.

Table 3.3: Maximum absolute errors of problem 3 for several Δt values with $N = 32$

Δt	Maximum absolute error
0.1	0.0024
0.01	0.0025
0.001	0.0025
0.0001	0.0025

It can be seen from the table that there is no significant difference between the choice of Δt but Δt=0.1 is slightly better. Therefore in the proceeding computations of this problem we use

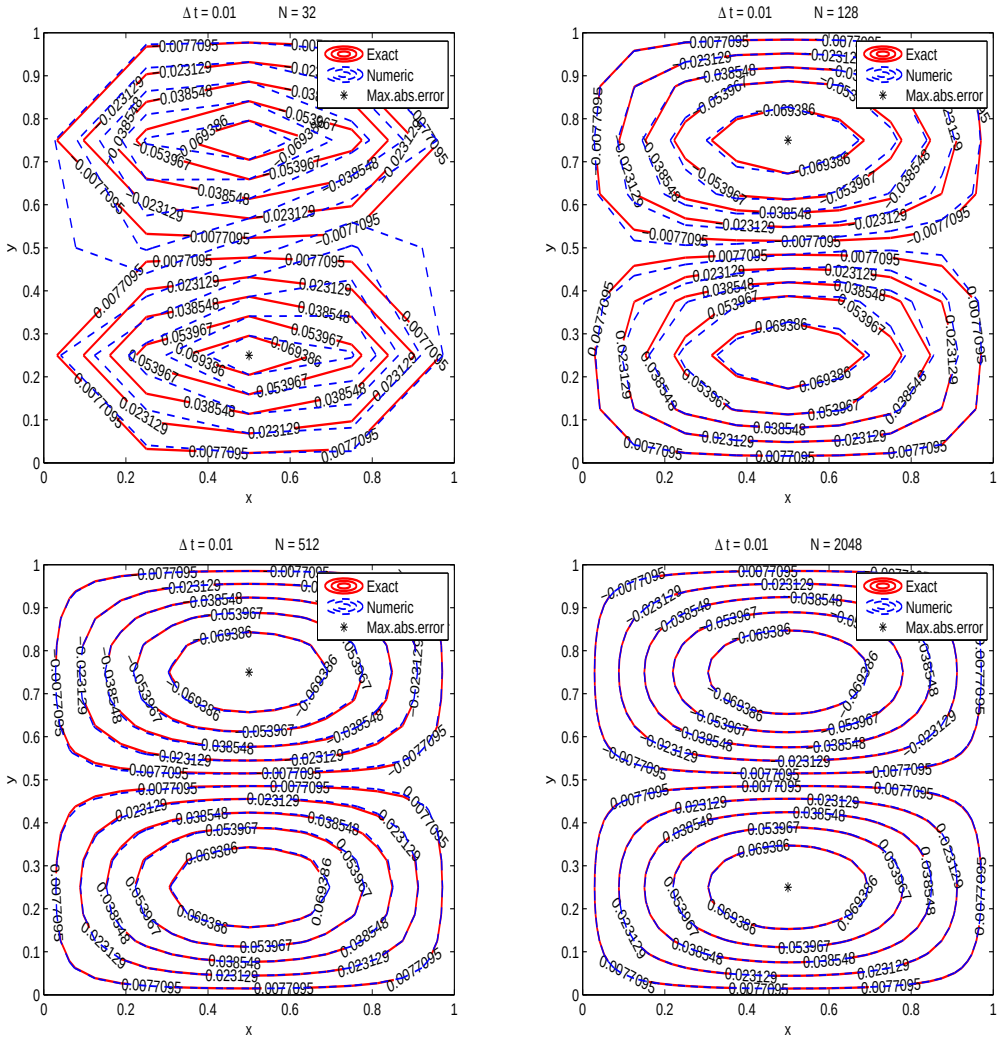

Figure 3.3: Contour plots of the exact solution and the finite element solution of problem 2 at $t = 0.05$

$\Delta t = 0.1$. Next, we take $N = 32$, 128, 512 and 2048. Once again we compare the maximum absolute error at time $t = 1$. The results are given in Table 3.4.

Table 3.4: Maximum absolute errors of problem 3 for several N values with $\Delta t = 0.1$

N	Maximum absolute error
32	0.0024
128	5.5757e-004
512	1.1761e-004
2048	2.3340e-004

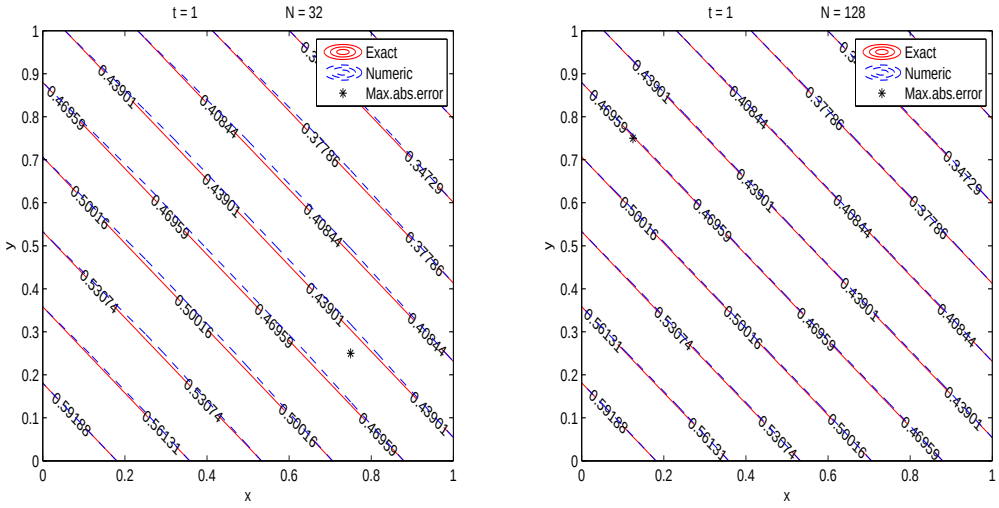

Figure 3.4: The exact solution and the finite element solution of problem 3 at t=1 using $\Delta t = 0.1$ and N=32 and 128

We see that increasing N from 32 to 128 decreases the error considerably. However, there is no significant difference between N=128 and N=512. Moreover, using 2048 elements cause a loss of accuracy compared to 512 for this problem. Figure 3.4 compares the contour plots of the exact solution and finite element solution at $t = 1$ using $N = 32$ and 128. We see from the figure that $N = 32$ is not enough, however when $N = 128$ the levels of the exact solution and the finite element solution coincide. We can conclude from these results that this problem is solved accurately with $\Delta t = 0.1$ and $N = 128$ for $t = 1$.

Now, we proceed to investigate the steady state solution of this problem. We take the middle point of the problem domain and check where the absolute difference between two solution values at consecutive time levels is less than the specified tolerance. The steady state time is $t = 13.9$ when tolerance is set to 10^{-4}. Therefore, we plot the exact solution and the finite element solution at the point $(0.5, 0.5)$ in the time interval [0,20] in Figure 3.5. The numerical solution is obtained using $\Delta t = 0.1$ and $N = 128$. We observe from this figure that the finite element solution agrees very well with the exact solution. It can also be deduced that the steady state is reached about $t = 14$ and the steady state solution of $u(0.5, 0.5, t)$ is 1.

3.2.4 Problem 4 : Diffusion-advection problem

The time-dependent diffusion-advection equation is

$$\frac{\partial u}{\partial t} - \frac{1}{2}\left(\frac{\partial^2 u}{\partial x^2} + \frac{\partial^2 u}{\partial y^2}\right) + \frac{1}{2}\left(\frac{\partial u}{\partial x} + \frac{\partial u}{\partial y}\right) = 0 \qquad \text{in } \Omega \times [0, T] \tag{3.27}$$

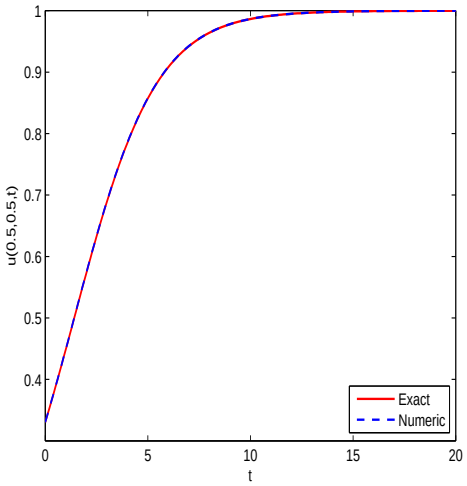

Figure 3.5: The exact solution and the finite element solution of problem 3 at (0.5,0.5) using $\Delta t = 0.1$ and N=128

where $\Omega = [0,1] \times [0,1]$. Dirichlet boundary conditions together with the initial condition are taken to be consistent with the exact solution which is given as [17]

$$u(x,y,t) = \frac{1}{\sqrt{s}} e^{-50(x+y-t)^2/s} \qquad \text{where } s = 1 + 200t. \tag{3.28}$$

As it was done before, we first fix $N = 32$ to seek for the best value of Δt. We take Δt= 0.1, 0.01, 0.001 and 0.0001 to test the solution at $t = 1$ and compare by looking at the maximum absolute error between the calculated solution and the exact solution. These maximum absolute errors are given in Table 3.5.

Table 3.5: Maximum absolute errors of problem 4 for several Δt values with $N = 32$

Δt	Maximum absolute error
0.1	0.0011
0.01	8.4182e-004
0.001	8.4184e-004
0.0001	8.4184e-004

It can be observed from this table that using $\Delta t = 0.01$ provides a considerable decrease in the error compared to using $\Delta t = 0.1$. There is not much of a difference in the errors when 0.01, 0.001 and 0.0001 are used for Δt. Therefore we conclude that it is convenient to take $\Delta t = 0.01$ for this problem. Next, we fix $\Delta t = 0.01$ and take N = 32, 128, 512 and 2048 to see how the

error changes with the number of elements used. Table 3.6 shows the maximum absolute errors between the exact solution and the finite element solution at $t = 1$.

Table 3.6: Maximum absolute errors of problem 4 for several $N = 32$ values with $\Delta t = 0.01$

N	Maximum absolute error
32	8.4182e-004
128	2.4401e-004
512	6.4659e-005
2048	2.1182e-005

This table shows that when N is increased the maximum absolute error is decreased. For a closer look, we print the contour plots of the exact solution and the numerical solution at $t = 1$ with several number of elements namely, 32, 128, 512 and 2048 in Figure 3.6.

It can be seen from this figure that $N = 32$ does not produce a good solution, $N = 128$ gives better result than $N = 32$. However, $N = 512$, $N = 2048$ improve the solution as it can be seen from Table 3.6 and Figure 3.6.

Figure 3.7 shows the plot of the exact solution and the finite element solution at the point (0.5, 0.5) using $N = 128$ and $\Delta t = 0.01$ in the time interval $[0, 25]$. We see from this plot that the steady state solution is reached, which is $u = 0$, at $t = 20$. Finally, Figure 3.8 shows the contour curves of the exact solution and the numerical solution at the steady state about $t = 20$ with $\Delta t = 0.01$ and several number of elements. We see from these figure plots that the steady state solution of this problem is obtained accurate enough with $N = 128$.

3.2.5 Problem 5 : System of reaction-diffusion equations

We now consider a system of reaction-diffusion equations in which the reaction terms are nonlinear functions. The equations are

$$\begin{cases} u_t - \nabla^2 u - u^2(1 - v^2) = f(x, y, t) \\ v_t - \nabla^2 v - v^2(1 - u^2) = g(x, y, t) \end{cases} \tag{3.29}$$

in $\Omega \times [0, T]$ where $\Omega = [0, 1] \times [0, 1]$.

The functions $f(x; y; t)$, $g(x; y; t)$ and the boundary and initial conditions are selected to

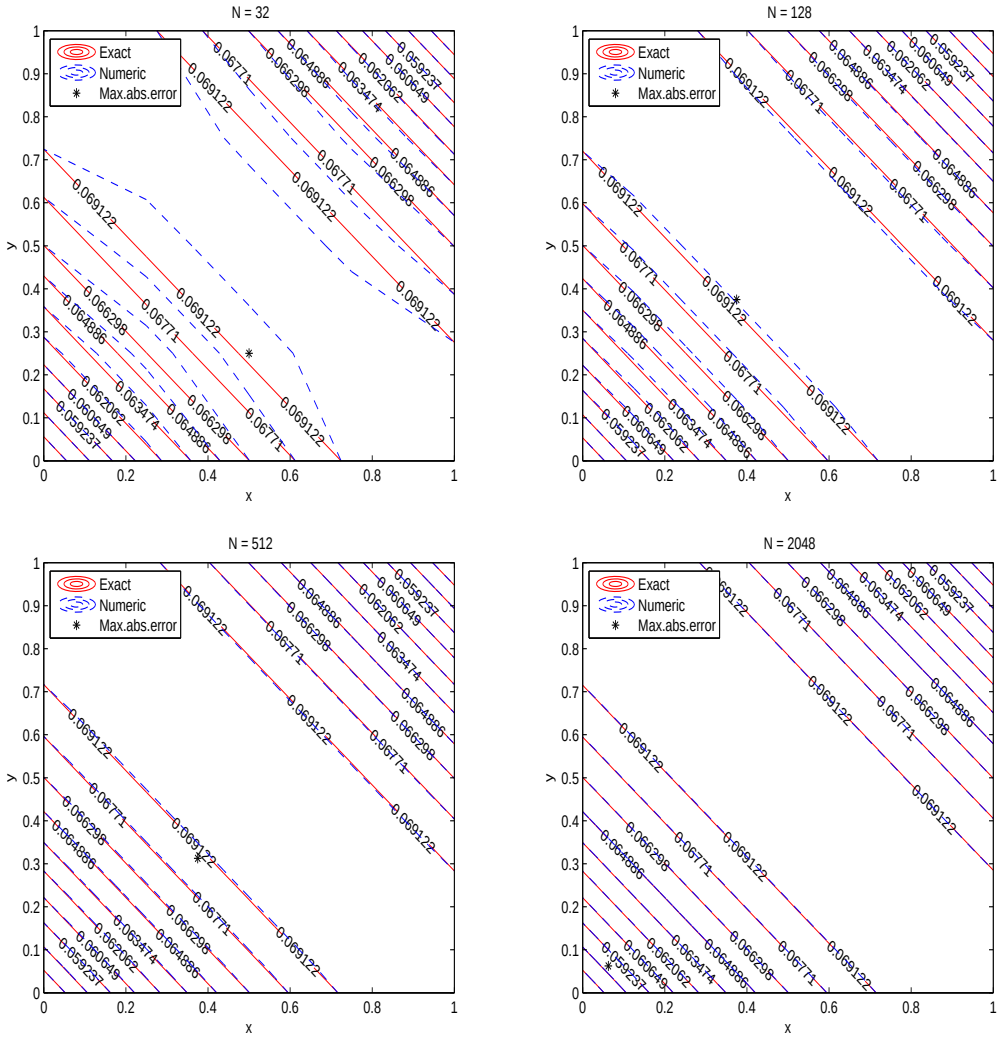

Figure 3.6: Contours of the exact solution and the finite element solution of problem 4 using $\Delta t = 0.01$

accommodate the exact solution which is given in [39]

$$\begin{cases} u(x,y,t) = e^{-t}\sin(x)\sin(y) \\ v(x,y,t) = e^{-2t}\sin(2x)\sin(2y). \end{cases} \tag{3.30}$$

The system (3.29) contains two nonlinear reaction diffusion equations each of which is similar to the equation in problem 3. To find the solution to this system using finite element method, starting from the initial conditions given, we first obtain the solutions u_k and v_k at t_k then using u_k and v_k we compute u_{k+1} and v_{k+1} and so on.

As in [39] we compute the solution at $t = 1$ to compare the finite element method solution with the exact solution to this system. It can be observed from the exact solution that both u and v approach to 0 as t increases. First we take $N = 32$ and let Δt vary from 0.1 to 0.0001,

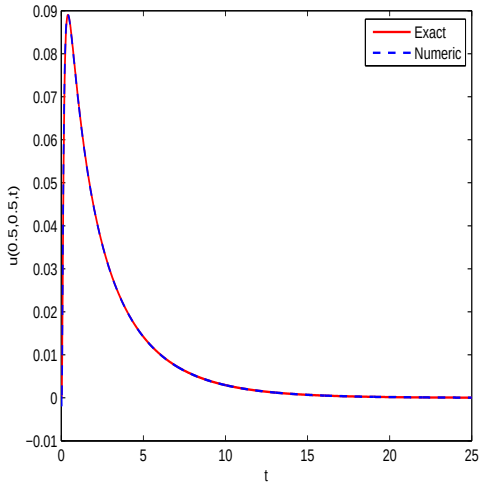

Figure 3.7: Plot of the exact solution and the finite element solution of problem 4, $N = 128$ and $\Delta t = 0.01$

the maximum errors are given in Table 3.7.

Table 3.7: Maximum absolute errors of problem 5 for several Δt values with $N = 32$

Δt	Maximum error of u	Maximum error of v
0.1	7.7399e-004	0.0072
0.01	0.0015	0.0026
0.001	0.0016	0.0032
0.0001	0.0016	0.0032

We see from this table that the smallest error occurs when $\Delta t = 0.1$ for u, however, for v it is when $\Delta t = 0.01$. As a second test, we take $N = 128$ and test the cases when $\Delta t = 0.1$, 0.01 and 0.001. The following table lists the results obtained.

Table 3.8: Maximum absolute errors of problem 5 for several Δt values with $N = 128$

Δt	Maximum error of u	Maximum error of v
0.1	7.9074e-004	0.0099
0.01	4.5196e-004	3.7530e-004
0.001	4.8957e-004	8.3550e-004

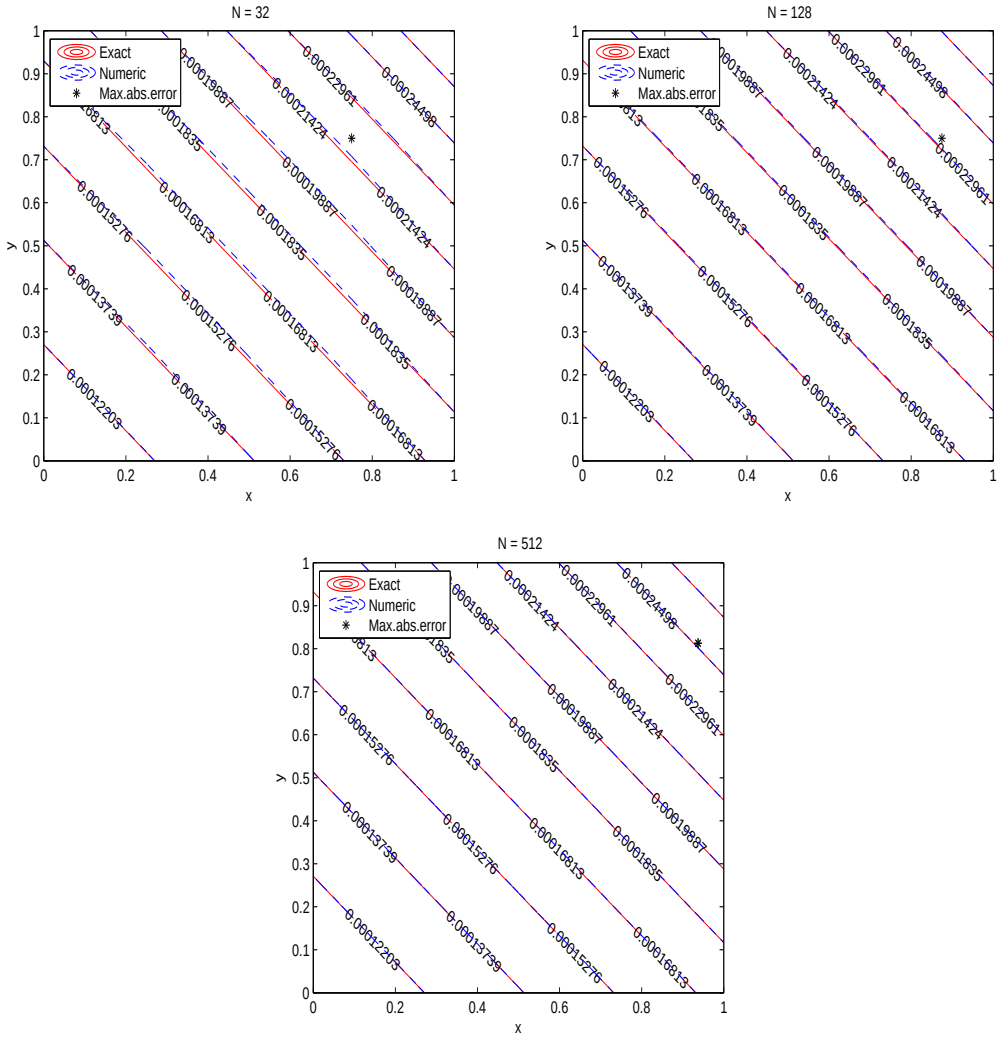

Figure 3.8: Contours of the exact solution and the finite element solution of problem 4 at steady state using $\Delta t = 0.01$

In Table 3.8, we see that the smallest error both for u and v occurs when Δt=0.01. Therefore to solve this problem we take Δt=0.01 and $N = 128$. Figure 3.9 and Figure 3.10 show the solutions at $t = 1$ using $N = 32$ and $N = 128$ respectively. It can be seen that $N = 128$ solves the system accurately, both u and v solutions which are obtained using finite element method, agree very well with the exact solution.

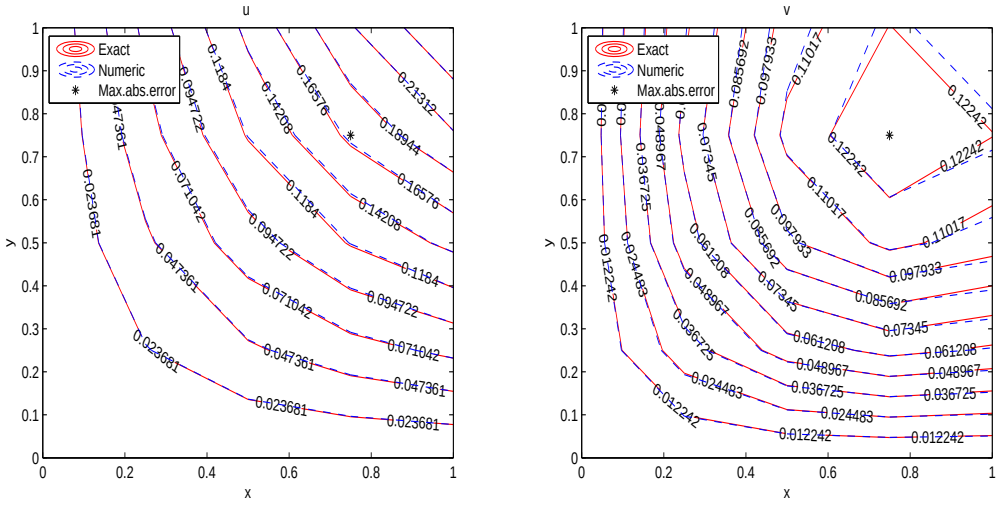

Figure 3.9: Contours of the exact solution and the finite element solution of problem 5 at $t = 1$, $\Delta t = 0.01$ and $N = 32$

3.2.6 Problem 6 : Reaction-diffusion system

The nonlinear reaction-diffusion system considered is

$$\begin{cases} \dfrac{\partial u}{\partial t} = \dfrac{1}{500}\nabla^2 u + 1 + u^2 v - \dfrac{3}{2}u \\ \\ \dfrac{\partial v}{\partial t} = \dfrac{1}{500}\nabla^2 v + \dfrac{1}{2}u - u^2 v \end{cases} \tag{3.31}$$

in $\Omega \times [0, T]$ where $\Omega = [0, 1] \times [0, 1]$.

The initial conditions are $u(x, y, 0) = \dfrac{1}{2}x^2 - \dfrac{1}{3}x^3$ and $v(x, y, 0) = \dfrac{1}{2}y^2 - \dfrac{1}{3}y^3$ and the boundary conditions are

$$\left(\frac{\partial u}{\partial x}, \frac{\partial v}{\partial x}\right) = (0, 0) \quad \text{on } x = 0, 1\ , \quad 0 < y < 1,$$
$$\left(\frac{\partial u}{\partial y}, \frac{\partial v}{\partial y}\right) = (0, 0) \quad \text{on } y = 0, 1\ , \quad 0 < x < 1.$$

There is no exact solution given to this problem. However, it is reported in [3] that the solution (u, v) to this system approaches to $(1, 1/2)$ as t increases. Therefore, to observe this consistency, we print the surface plots of u and v at $t = 0$, 1, 2 and 5. The finite element solutions are obtained taking $\Delta t = 0.01$ and $N = 128$. Figure 3.11 shows u and Figure 3.12 shows v level curves. We can easily see from these figures that $(u, v) \to (1, 1/2)$ as t increases which is expected and which shows this system is solved properly using finite element method. Additionally, for a closer look, we once again pick the middle node, that is $(0.5, 0.5)$ to observe

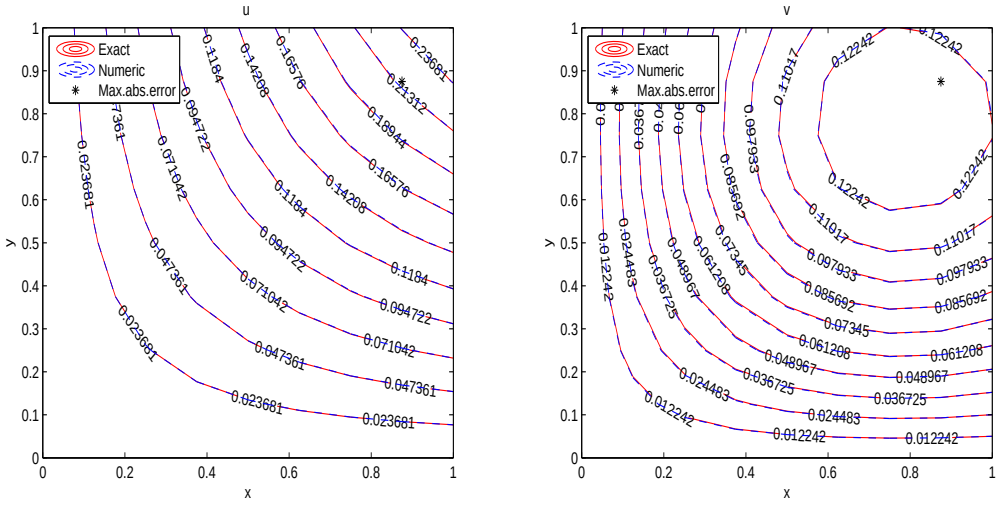

Figure 3.10: Contours of the exact solution and the finite element solution of problem 5 at $t = 1$, $\Delta t = 0.01$ and $N = 128$

the solutions on this node. In Figure 3.13 we plot u and v in the time interval $[0, 10]$. We see that (u, v) at the middle node approach to $(1, 1/2)$.

3.2.7 Problem 7 : Reaction-diffusion Brusselator system

The chemical system

$$\begin{aligned} B_{in} &\longrightarrow X \\ A_{in} + X &\longrightarrow Y + D \\ 2X + Y &\longrightarrow 3X \\ X &\longrightarrow E \end{aligned} \tag{3.32}$$

considered in [48] is known as Brusselator system. A_{in} and B_{in} are input chemicals, D and E are output chemicals and X and Y are intermediates. The kinetic equations associated with (3.32) are given by

$$\begin{aligned} \frac{\partial X}{\partial t} &= k_1 B + k_2 X^2 Y - k_3 A X - k_4 X + D_x \nabla^2 X \\ \frac{\partial Y}{\partial t} &= k_3 A X - k_2 X^2 Y + D_y \nabla^2 Y \end{aligned} \tag{3.33}$$

where k_1, k_2, k_3 and k_4 are rate constants.

Letting $u = u(x, y, t)$ and $v = v(x, y, t)$ represent the concentrations of two reaction products at time t, A and B are constant concentrations of two input reactants and $D_x = D_y = \alpha$. The nonlinear partial differential equations associated with the Brusselator system are given by (see, [48])

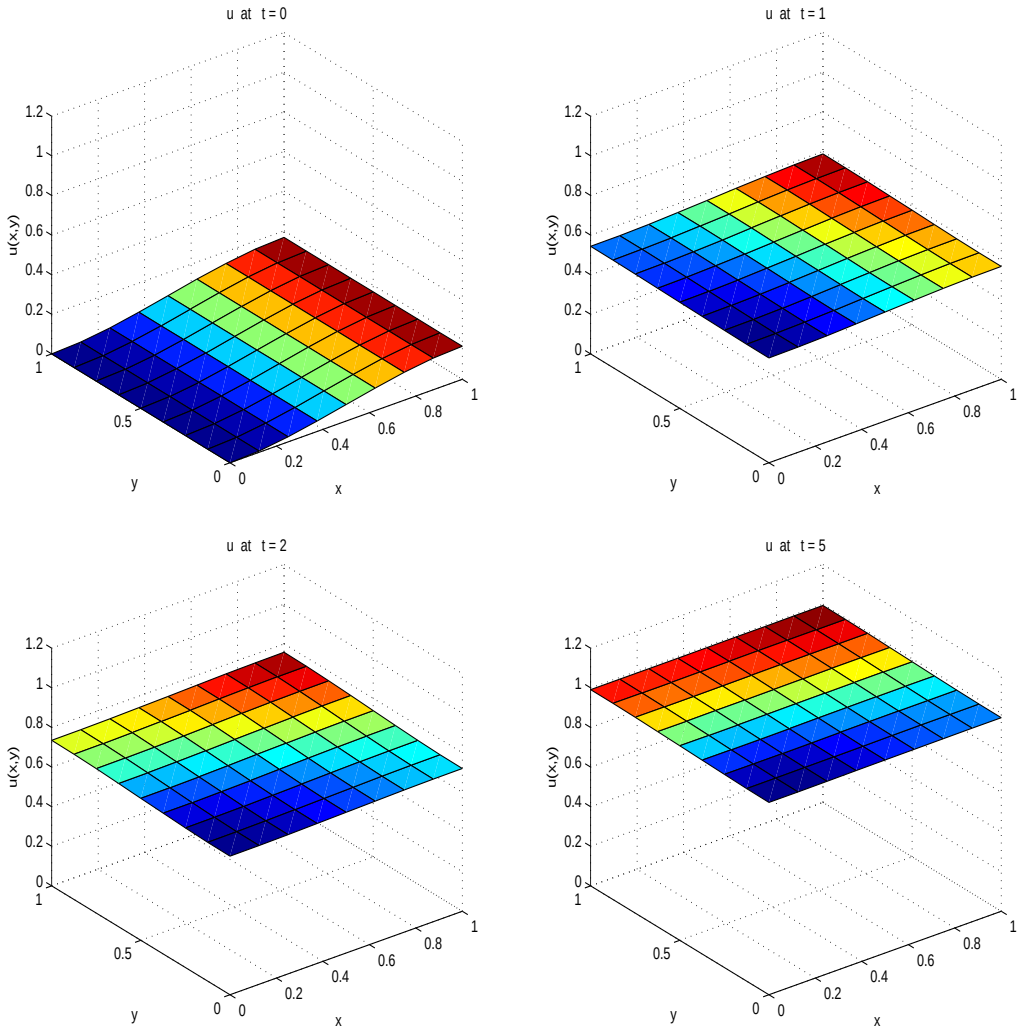

Figure 3.11: u at t=0, 1, 2 and 5 using $\Delta t = 0.01$ and $N = 128$ for problem 6

$$\begin{aligned} \frac{\partial u}{\partial t} &= B + u^2 v - (A+1)u + \alpha \nabla^2 u \\ \frac{\partial v}{\partial t} &= Au - u^2 v + \alpha \nabla^2 v \end{aligned} \tag{3.34}$$

in $0 < x, y < L$ where L is the reactor length. The equations are subject to Neumann boundary conditions given by

$$\left(\frac{\partial u}{\partial x}, \frac{\partial v}{\partial x}\right) = (0,0) \text{ on } x = 0, L \text{ where } 0 < y < L,$$
$$\left(\frac{\partial u}{\partial y}, \frac{\partial v}{\partial y}\right) = (0,0) \text{ on } y = 0, L \text{ where } 0 < x < L.$$

The initial conditions are given as $u(x, y, 0) = 2 + 0.25y$ and $v(x, y, 0) = 1 + 0.8x$. We take

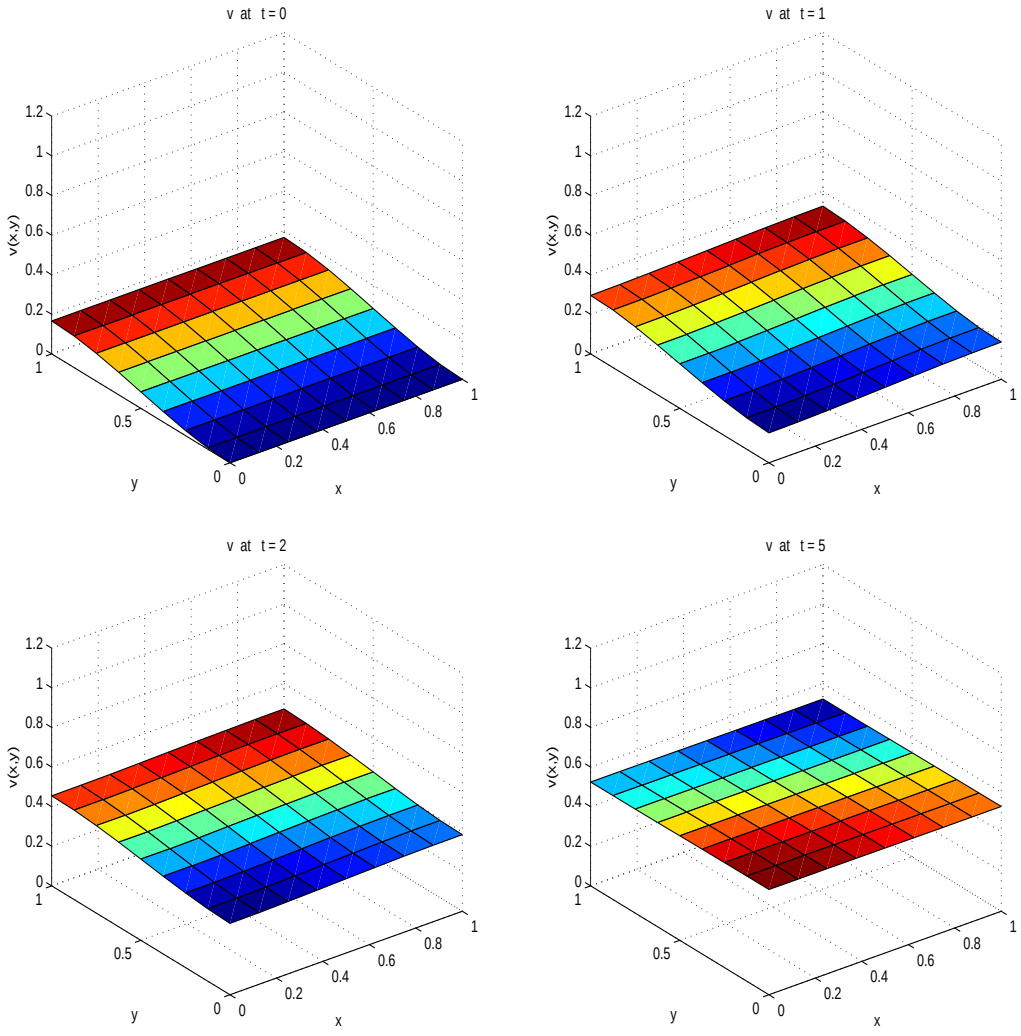

Figure 3.12: v at t=0, 1, 2 and 5 using $\Delta t = 0.01$ and $N = 128$ for problem 6

$L = 1$, $A = 1$, $B = 2$ and $\alpha = 0.002$, same as in [48], and compute the solution at $t = 5$ to compare the profiles of u and v given there. We have used the finite element method with $N = 128$ and $\Delta t = 0.01$. Figure 3.14 shows u obtained by finite element method proposed in the thesis and the behavior of u is in well accordance with the behavior given on pages 313 and 314 in [48]. And similarly Figure 3.15 shows v. It is reported in [48] that for the selected parameters of this system, the concentration profiles of u and v converge to $(u, v) = (2, 1/2)$. In Figure 3.16 we plot u and v at t=10 and it can be seen from this figure that u and v converge to $(u, v) = (2, 1/2)$ on the whole domain of the problem. This shows that the finite element method solved this system accurately with $N = 128$ and $\Delta t = 0.01$. Finally, the last figure of this problem, Figure 3.17, depicts u and v at the middle point in the time interval [0,10]. From these plots too we see that u converges to 2 and v converges to 0.5 as t increases.

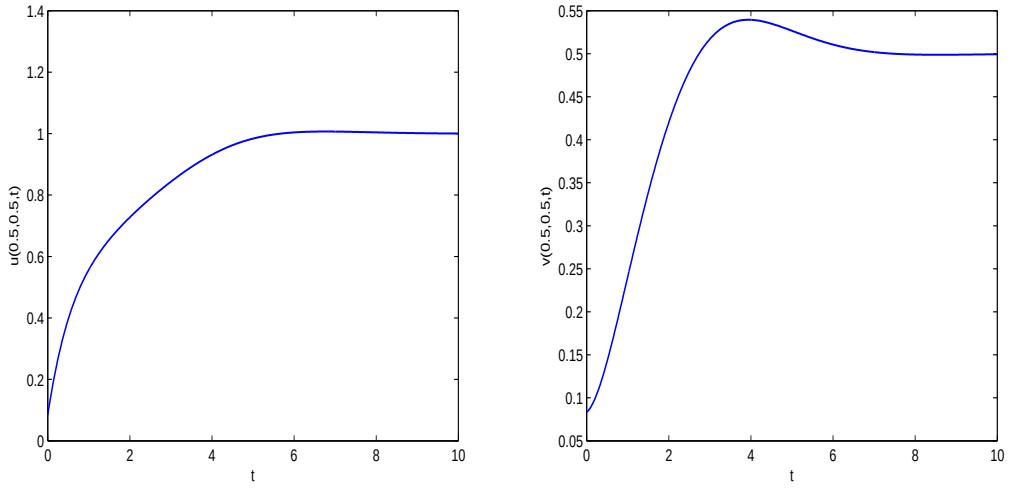

Figure 3.13: $u(0.5, 0.5, t)$ and $v(0.5, 0.5, t)$ in the time interval [0,10] for problem 6

3.2.8 Problem 8 : Reaction-diffusion-advection problem

The reaction-diffusion-advection equation is

$$\frac{\partial u}{\partial t} - 10^{-8}\left(\frac{\partial^2 u}{\partial x^2} + \frac{\partial^2 u}{\partial y^2}\right) + 2\frac{\partial u}{\partial x} - \frac{\partial u}{\partial y} + u = f \qquad \text{in } \Omega \times [0, T] \tag{3.35}$$

where $\Omega = [0, 1] \times [0, 1]$. Dirichlet boundary conditions, the initial condition and the source function f are taken to be consistent with the exact solution which is given as [35]

$$u(x, y, t) = t^2 \cos(xy^2). \tag{3.36}$$

The diffusion constant of this problem is $\varepsilon = 10^{-8}$ and hence the problem is reaction and advection dominated. Therefore, we solve this problem using the stabilized FEM described in Section 3.1.1. We present the contour plots of the numerical solution obtained from stabilized FEM and the exact solution using $N = 128$ and $N = 512$ at time $t = 10$ in Figure 3.18. It can be seen from the figure that the stabilized FEM solution agrees well with the exact solution with $N = 512$. The problem does not have a steady state solution as the solution increases with time.

3.2.9 Problem 9 : A basic air pollution model

We consider the following reactions, which constitute a basic air pollution model [22, 49]

$$\begin{aligned} NO_2 + h\nu &\xrightarrow{k_1} NO + O(^3P) \\ O(^3P) + O_2 &\xrightarrow{k_2} O_3 \\ NO + O_3 &\xrightarrow{k_3} O_2 + NO_2. \end{aligned} \tag{3.37}$$

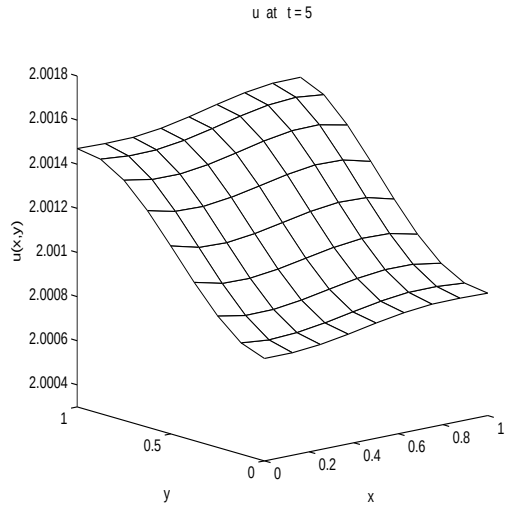

Figure 3.14: u at $t = 5$ of problem 7

In this reaction system, NO_2 is nitrogen dioxide, NO is nitrogen oxide, $O(^3P)$ is atomic oxygen, O_2 is molecular oxygen and O_3 is ozone [45]. The term $h\nu$ in the first reaction indicates that this reaction is photochemical, that is, it depends on light. The constants k_1, k_2 and k_3 are the reaction coefficients.

Putting now $u_1 = [O(^3P)]$, $u_2 = [NO]$, $u_3 = [NO_2]$ and $u_4 = [O_3]$ to denote the concentrations, the associated ODE system reads [49]

$$\begin{aligned}
\frac{du_1}{dt} &= k_1 u_3 - k_2 u_1 \\
\frac{du_2}{dt} &= k_1 u_3 - k_3 u_2 u_4 + s_2 \\
\frac{du_3}{dt} &= k_3 u_2 u_4 - k_1 u_3 \\
\frac{du_4}{dt} &= k_2 u_1 - k_3 u_2 u_4.
\end{aligned} \tag{3.38}$$

The unit for time here is seconds and for concentrations number of molecules per cm^3. As a natural assumption, oxygen concentration is taken to be constant, and a source s_2 is added for NO in the second equation. The initial concentrations are

$$\begin{aligned}
u_1 &= 0 \\
u_2 &= 1.3 \times 10^8 \\
u_3 &= 5.0 \times 10^{11} \\
u_4 &= 8.0 \times 10^{11}
\end{aligned} \tag{3.39}$$

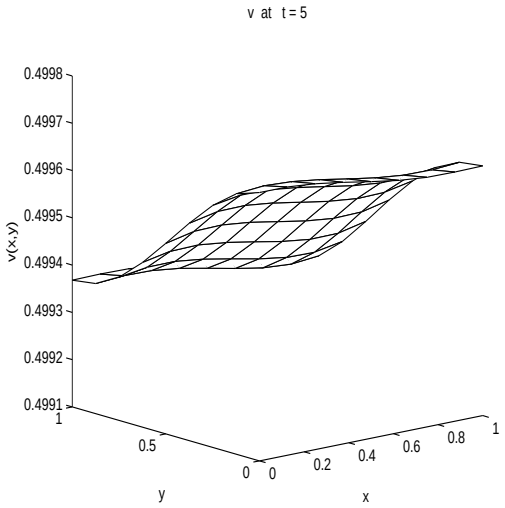

Figure 3.15: v at $t = 5$ of problem 7

and $s_2 = 10^6$. The reaction coefficients are given as

$$\begin{aligned} &k_3 = 10^{-16} \\ &k_2 = 10^5 \\ &k_1 = 10^{-40} \ \text{(night time)} \ , \ \ k_1 = 10^{-5} e^{7sec(t)} \ \text{(day time)} \end{aligned} \tag{3.40}$$

where

$$sec(t) = \left(\sin\left(\frac{\pi}{16}\left(t_h - 4\right)\right)\right)^{0.2}, \ \ t_h = th - 24\lfloor th/24 \rfloor, \ \ th = t/3600. \tag{3.41}$$

The daytime is taken to be between 4 o'clock in the morning and 8 o'clock in the evening. The concentration values and reaction coefficients more or less approximate their counterparts used in real models. Because oxygen is held constant, k_2 contains the total number of O_2 molecules per cm^3 and is therefore much larger than k_1 and k_3, [49].

Introducing spatial diffusion effect to the system (3.38) on a domain $(x, y) \in (-L, L)^2$ and a source term $S(x, y) = s_2 e^{-40(x^2+y^2)/L^2}$ with homogeneous Neumann boundary conditions where $L = 400$, the system [22]

$$\begin{aligned} \frac{\partial u_1}{\partial t} &= \nabla^2 u_1 + k_1 u_3 - k_2 u_1 + S(x, y) \\ \frac{\partial u_2}{\partial t} &= \nabla^2 u_2 + k_1 u_3 - k_3 u_2 u_4 + s_2 + S(x, y) \\ \frac{\partial u_3}{\partial t} &= \nabla^2 u_3 + k_3 u_2 u_4 - k_1 u_3 + S(x, y) \\ \frac{\partial u_4}{\partial t} &= \nabla^2 u_4 + k_2 u_1 - k_3 u_2 u_4 + S(x, y) \end{aligned} \tag{3.42}$$

is obtained.

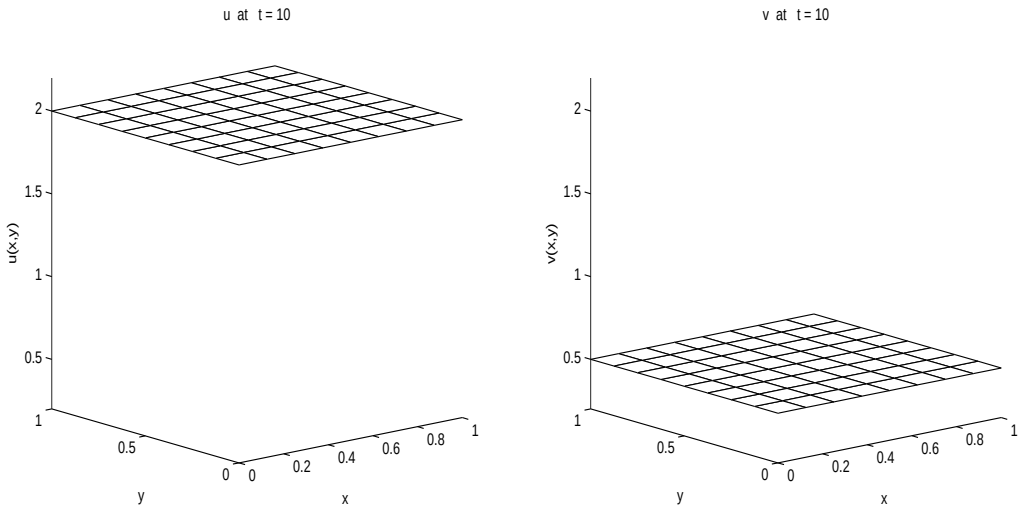

Figure 3.16: Solution to problem 7, u and v at $t = 10$ obtained by finite element method with $N = 128$ and $\Delta t = 0.01$

We solve this problem using the stabilized FEM with $N = 2048$ to obtain an observation of the concentrations of the model on the problem domain. We present the solution at $t = 3\times10^5$ as in [22] in Figure 3.19. We see from the figure that u_1, u_2 and u_4 are increasing , u_3 is decreasing by time. The peaks are at the center due to the source $S(x, y)$ added to the model for u_1, u_2, u_3 and u_4. Note that u_4 has a minimum at the center. As time increases the concentrations increase from the center to the boundaries.

From the test problems considered in this chapter we see that there is no need to use very small Δt in the computations. Similar to time-independent problems, for transient problems too, as ε gets smaller the FEM needs more elements to obtain accurate solutions. The solutions to the problems (1)-(7) are obtained by the standard FEM making use of Crank-Nicolson scheme for the temporal discretization. The solution to the problems (8) and (9) are obtained by the stabilized FEM because of the advection and/or reaction dominance.

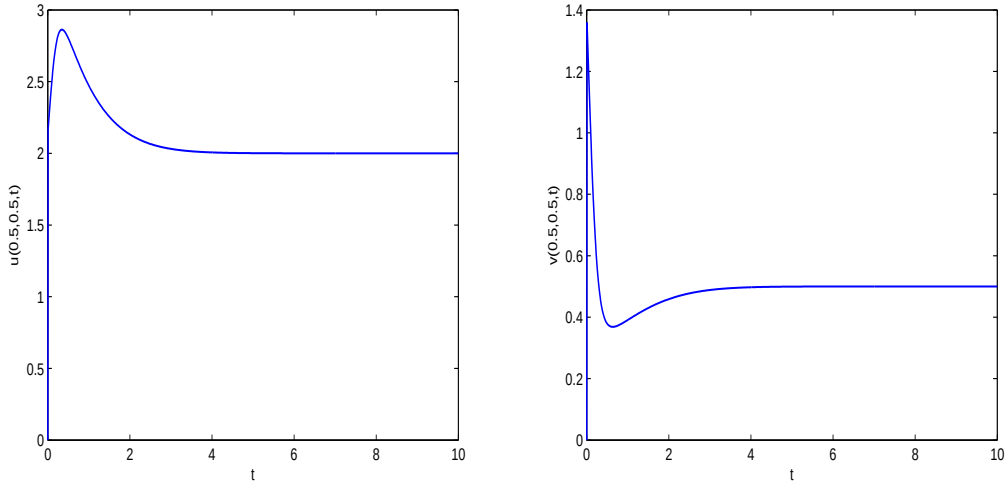

Figure 3.17: $u(0.5, 0.5, t)$ and $v(0.5, 0.5, t)$ of problem 7 where t $\in [0, 10]$

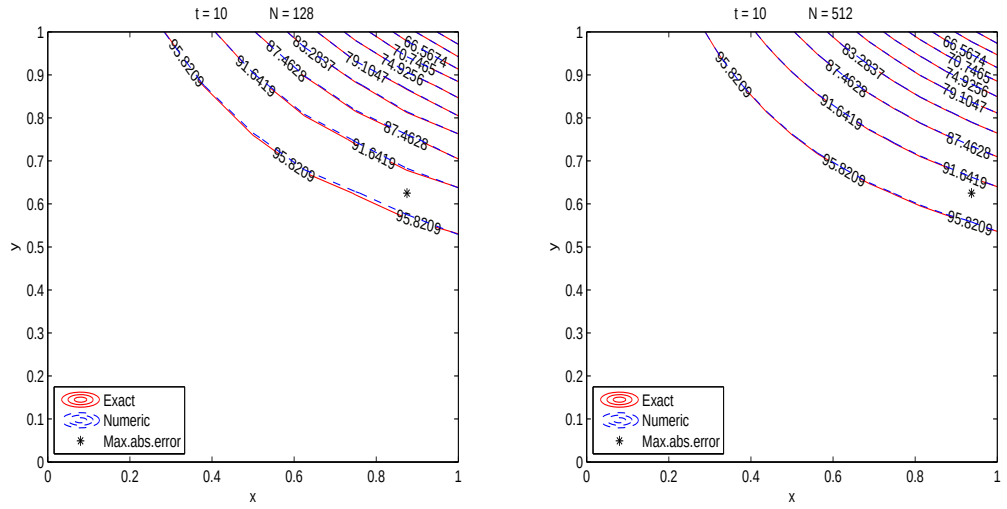

Figure 3.18: Contour plots of problem 8 at $t = 10$ with $N = 128$ and $N = 512$

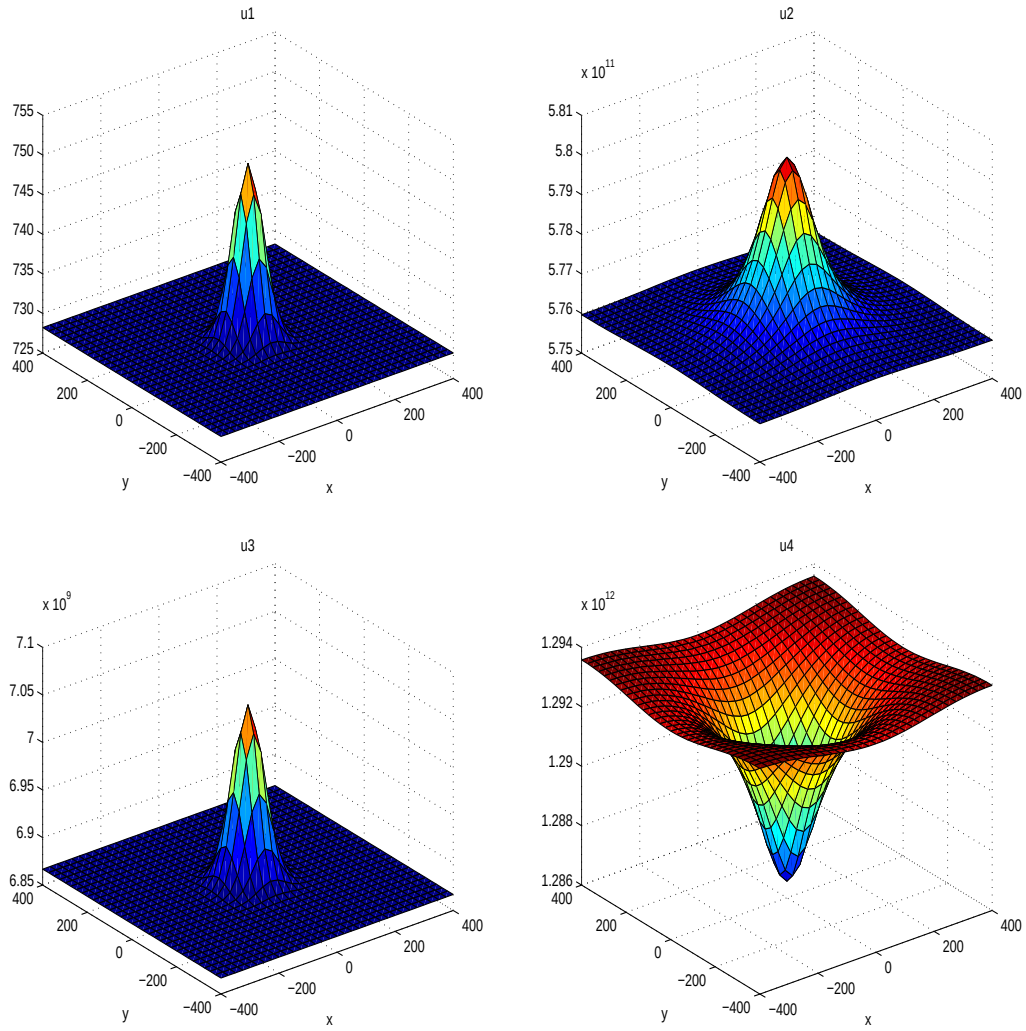

Figure 3.19: Solution of problem 9 at $t = 3 \times 10^5$ with $N = 2048$

Chapter 4

Conclusion

In this thesis, general mathematical description of an air pollution model is given. Reaction-diffusion-advection (RDA) equations which are the governing equations of some air pollution models are described. The finite element method (FEM) is applied for solving RDA equations. The domain is discretized by using linear triangular elements. Numerical experiments presented in the study show that the standard FEM introduces nonphysical oscillations in the solution for reaction or advection dominated problems. An adaptive scheme which is based on adding to the variational formulation some numerical diffusion terms to stabilize the finite element solution is described. The stabilized FEM is shown to avoid the oscillations in the solution produced by the standard FEM. The unconditionally stable Crank-Nicolson scheme is used for temporal dicsretization in transient RDA problems. Thus, the use of very small time increment is avoided. The stabilization for transient RDA problems improves the solution too, however it is not that effective as in the steady case.

Numerical results are obtained for some steady and transient RDA problems. As the diffusivity constant (advection or reaction dominance) gets smaller, standard Galerkin FEM method needs more finite elements to take for steady and unsteady problems. For very small diffusivity constant stabilization is necessary to solve the RDA equations. Solutions of the problems are visualized in terms of graphics comparing with the exact solutions whenever possible. One application in the air pollution modeling is also given. It is found that the pollution source introduces peaks at the center region and these peaks are spread as time increases.

Air pollution models containing large number of pollutants result in mathematical models with large number of equations. In fact, in many cases the large air pollution models are not tractable at all unless the numerical algorithms are sufficiently fast. Generally, one is advised to use parallel computation for large air pollution problems.

References

[1] Alexandrov V N and Zlatev Z. Using parallel Monte Carlo methods in large-scale air pollution modelling. TextitM. Bubak et al. (Eds.): ICCS 2004, LNCS 3039 Springer-Verlag Berlin Heidelberg (2004) 491-498.

[2] Alexandrov V N, Owczarz W, Thomson P G and Zlatev Z. Parallel runs of a large air pollution model on a grid of Sun computers. *Mathematics and Computers in Simulation* 65 (2004) 557-577.

[3] Ang W T. The two-dimensional reaction-diffusion Brusselator system: a dual-reciprocity boundary element solution. *Engineering Analysis with Boundary Elements* 27 (2003) 897-903.

[4] Araya R, Behrens E and Rodriguez R. An adaptive stabilized finite element scheme for the advection-reaction-diffusion equation. *Applied Numerical Mathematics* 54 (2005) 491-503.

[5] Asensio M I, Ayuso B and Sangalli G. Coupling stabilized finite element methods with finite difference time integration for advection-diffusion-reaction problems. *Computer Methods in Applied Mechanics and Engineering* 196 (2007) 3475-3491.

[6] Aydin S H. The finite element method over a simple stabilizing grid applied to fluid flow problems. *Ph.D.Thesis, IAM, METU* (2008).

[7] Baumann C E and Oden J T. A discontinuous hp finite element method for convection-diffusion problems. *Computer Methods in Applied Mechanics and Engineering* 175 (1999). 311-341

[8] Bermejo R and Carpio J. An adaptive finite element semi-Lagrangian implicit-explicit Runge-Kutta-Chebyshev method for convection dominated reaction-diffusion problems. *Applied Numerical Mathematics* 58 (2008) 16-39.

[9] Bozkaya C. Least-squares differential quadrature time integration scheme in the dual reciprocity boundary element method solution of diffusiveconvective problems. *Engineering Analysis with Boundary Elements* 31 (2007) 83-93.

[10] Brezzi F, Bristeau M O, Franca L P, Mallet M and Roge G. A relationship between stabilized finite element methods and the Galerkin method with bubble functions. *Computer Methods in Applied Mechanics and Engineering* 96 (1992) 117-129.

[11] Brezzi F and Russo A, Choosing bubbles for advection-diffusion problems. *Mathematical Models and Methods in Applied Sciences* 4 (1994) 571-587.

[12] Brooks A N and Hughes T J R. Streamline upwind Petrov-Galerkin formulation for convection dominated flows with particular emphasis on the incompressible Navier-Stokes equations. *Computer Methods in Applied Mechanics and Engineering.* 32 (1982) 199-259.

[13] Burman E and Ern A. Stabilized galerkin approximation of convection-diffusion-reaction equations: Discrete maximum principle and convergence. *Mathematics Of Computation* Vol.74, No.252 (2005) 1637-1652.

[14] Caliari M, Vianello M and Bergamaschi L. The LEM exponential integrator for advection-diffusion-reaction equations. *Journal Of Computational and Applied Mathematics*(2006).

[15] Cannon J R and Lin Y. A priori L^2 error estimates for finite element methods for nonlinear diffusion equations with memory. *SIAM Journal on Numerical Analysis.* (1990) 595-607.

[16] Chawla M M, Al-Zanaidi M A and Al-Aslab M G. Extended one-step time-integration schemes for convection-diffusion equations. *Computers and Mathematics with Applications* 39 (2000) 71-84.

[17] Chawla M M and Al-Zanaidi M A. An Extended trapezoidal formula for the diffusion equation in two space simensions. *Computers and Mathematics with Applications* 42 (2001) 157-168.

[18] Chou C S, Zhang Y T, Zhao R and Nie Q. Numerical methods for stiff reaction-diffusion systems. *Discrete and Continuous Dynamical Systems-Series B* Vol.7, No.3 (2007).

[19] Codina R. Comparison of some finite element methods for solving the diffusion-convection-reaction equation. *Computer Methods in Applied Mechanics and Engineering* 156 (1998) 185-210.

[20] Dan D, Mueller C, Chen K and Glazier JA. Solving the advection-diffusion equations in biological contexts using the cellular Potts model. *Physical Review E 72, 041909* (2005).

[21] Dimov I, Georgiev K, Ostromsky Tz and Zlatev Z. Computational challenges in the numerical treatment of large air pollution models. *Ecological Modelling* 179 (2004) 187203.

[22] Dupros F, Garbey M and Fitzgibbon W E. A filtering technique for system of reaction-diffusion equations . *International Journal for Numerical Methods in Fluids* 52 (2006) 1-29.

[23] Fang Q. Convergence of finite difference methods for convection-diffusion problems with singular solutions. *Journal of Computational and Applied Mathematics*152 (2003) 119-131.

[24] Faugeras B, Maury O. An advection-diffusion-reaction size-structured fish population dynamics model combined with a statistical parameter estimation procedure. *Mathematical Biosciences and Engineering* (2005).

[25] Franca L P, Frey S L and Hughes T J R. Stabilized finite element methods: I. Application to the advective-diffusive model. *Computer Methods in Applied Mechanics and Engineering* 95 (1992) 253-276.

[26] Franca L P and Farhat C. Bubble functions prompt unusual stabilized finite element methods. *Computer Methods in Applied Mechanics and Engineering* 123 (1995) 299-308.

[27] Franca L P and Russo A. Deriving upwinding, mass lumping and selective reduced integration by residual-free bubbles. *Applied Mathematics Letters* 9 (1996) 83-88.

[28] Franca L P, Nesliturk A and Stynes M. On the stability of residual-free bubbles for convection-diffusion problems and their approximation by a two-level finite element method. *Computer Methods in Applied Mechanics and Engineering* 166 (1998) 35-49.

[29] Franca L P and Macedo A P. A two-level finite element method and its application to the Helmholtz equation. *International Journal for Numerical Methods in Engineering* 43 (1998) 23-32.

[30] Franca L P and Valentin F. On an improved unusual stabilized finite element method for the advective-reactive-diffusive equation. *Computer Methods in Applied Mechanics and Engineering* 190 (2000) 1785-1800.

[31] Franca L P, Hauke G and Masud A. Revisiting stabilized finite element methods for the advective-diffusive equation. *Computer Methods in Applied Mechanics and Engineering* 195 (2006) 1560-1572.

[32] Gracia J L and Lisbona F J. A uniformly convergent scheme for a system of reaction-diffusion equations. *Journal of Computational and Applied Mathematics* 206 (2007) 1-16.

[33] Gravemeier V and Wall W A. A 'divide-and-conquer' spatial and temporal multiscale method for transient convection-diffusion-reaction equations. *International Journal for Numerical Methods in Fluids* (2007) 779-804.

[34] Hughes T J R, Franca L P and Hulbert G M. A new finite element formulation for computational fluid dynamics: VIII. The Galerkin-least-squares method for advective-diffusive equations. *Computer Methods in Applied Mechanics and Engineering* 73 (1989) 173-189.

[35] John V, Kaya S and Layton W. A two-level variational multiscale method for convection-dominated convection-diffusion equations. *Computer Methods in Applied Mechanics and Engineering* 195 (2006) 4594-4603.

[36] Knobloch P. Improvements of the Mizukami-Hughes method for convection-diffusion equations. *Computer Methods in Applied Mechanics and Engineering* 196 (2006) 579-594.

[37] Lanser D and Verwer J G. Analysis of operator splitting for advection-diffusion-reaction problems from air pollution modelling. *Journal of Computational and Applied Mathematics* 111 (1999) 201-216.

[38] Li J and Navon I M. Uniformly convergent finite element methods for singularly perturbed elliptic boundary value problems: convection-diffusion type. *Computer Methods in Applied Mechanics and Engineering* 162 (1998) 49-78.

[39] Liao W, Zhu J and Khaliq Q M. An efficient high-order algorithm for solving systems of reaction-diffusion equations. *Numerical Methods for Partial Differential Equations* 18 (2002) 340-354.

[40] Long P E and Pepper D W. An examination of some simple numerical schemes for calculating scalar advection. *Journal of Applied Meteorology* (1980).

[41] Marchuk G I. Mathematical models for environmental problems. *Nauca,Moscow* (1982).

[42] Molenkamp C R. Accuracy of finite-difference methods applied to the advection equation. *Journal of Applied Meteorology* (1967).

[43] Reddy J N. An introduction to the finite element method. *The McGraw-Hill Companies* (2006).

[44] Simo J C, Armero F and Taylor C A. Stable and time-dissipative finite element methods for the incompressible Navier-Stokes equations in advection dominated flows. *International Journal for Numerical Methods in Engineering* 38 (1995) 1475-1506.

[45] Spee E J, Verwer J G, de Zeeuw P M, Blom J G and Hundsdorfer W. A numerical study for global atmospheric transport-chemistry problems. *Mathematics and Computers in Simulation* 48 (1998) 177-204.

[46] Tezduyar T E and Park Y J. Discontinuity-capturing finite element formulations for nonlinear convection-diffusion-reaction equations. *Computer Methods in Applied Mechanics and Engineering.* 59 (1986) 307-325.

[47] Tian Z F and Dai S Q. High-order compact exponential finite difference methods for convection-diffusion type problems. *Journal of Computational Physics* 220 (2007) 952-974.

[48] Twizell E H, Gumel A B and Cao Q.A second-order scheme for the Brusselator reaction-diffusion system . *Journal of Mathematical Chemistry* 26 (1999) 297-316.

[49] Verwer J G, Hundsdorfer W H and Blom J G. Numerical time integration for air pollution models. *Report MAS-R9825 November 1998, CWI* (1998).

[50] Zlatev Z. Computer Treatment of Large Air Pollution Models. *Kluwer Academic Publishers* (1995).